Course of Geodynamics

Dr. Magdala Tesauro

Course Outline:

1. Thermo-physical structure of the continental and oceanic crust
2. Thermo-physical structure of the continental lithosphere
3. **Thermo-physical structure of the oceanic lithosphere and oceanic ridges**
4. Strength and effective elastic thickness of the lithosphere
5. Plate tectonics and boundary forces
6. Hot spots, plumes, and convection
7. Subduction zones systems
8. Orogens formation and evolution
9. Sedimentary basins formation and evolution

Mid-Ocean Ridges

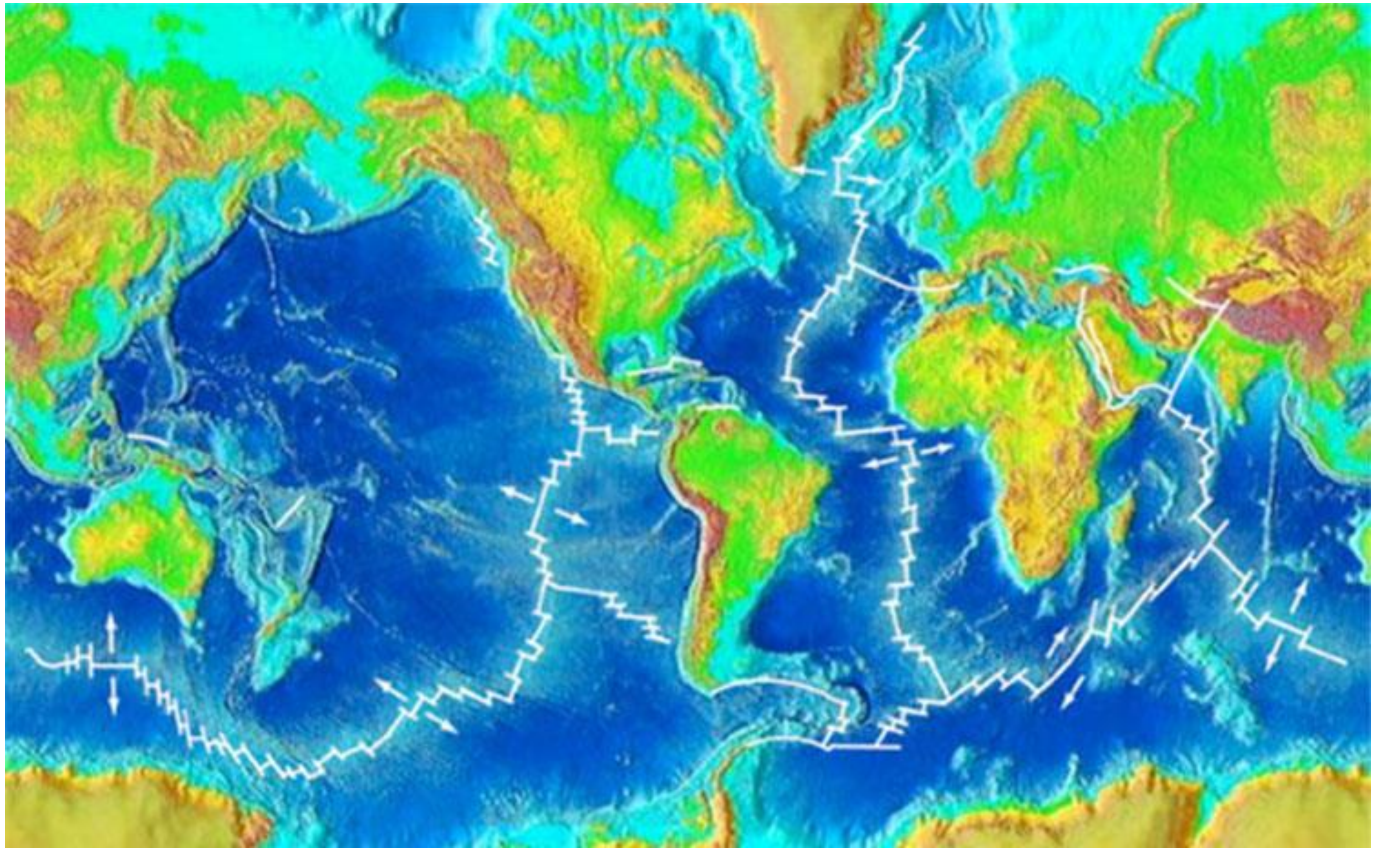

- A system of submarine mountains over 60000 km long, 1000-4000 km wide, 2500 deep, segmented by transform faults.
- More than 60 % of the magmatic rocks of the Earth are generated at the ridges (20 km^3yr^{-1}).
- Mid-Ocean ridges occupy a central position (e.g., in the Atlantic Ocean) if the ocean is bordered by passive continental margins, otherwise is shifted (e.g., in the Pacific Ocean) towards the direction of most rapid subduction.
- Spreading rates range from 15 $cmyr^{-1}$ (equatorial Pacific) to 1 $cmyr^{-1}$ (Artic region).
- Earthquakes, related to rising magma, occur along the ridge (extensional regime) and transform faults (strike slip).

Mid-Ocean Ridges, petrology, topography, and gravity anomalies

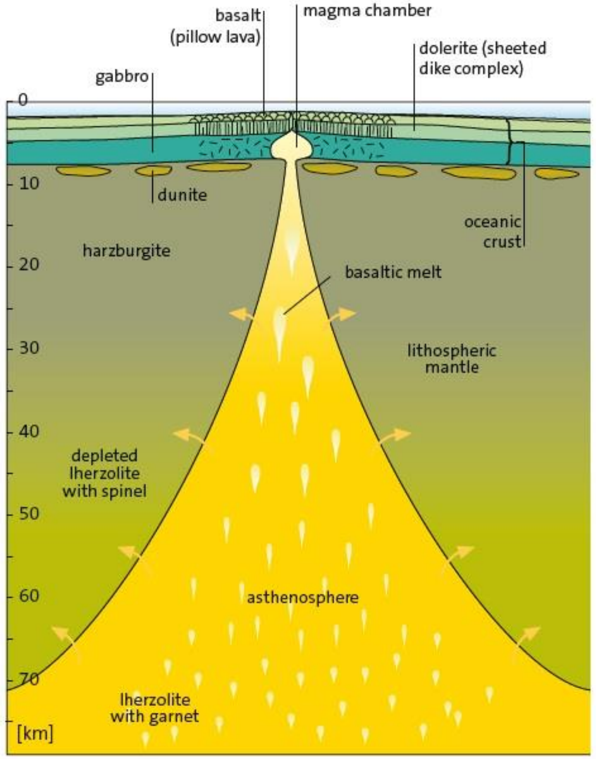

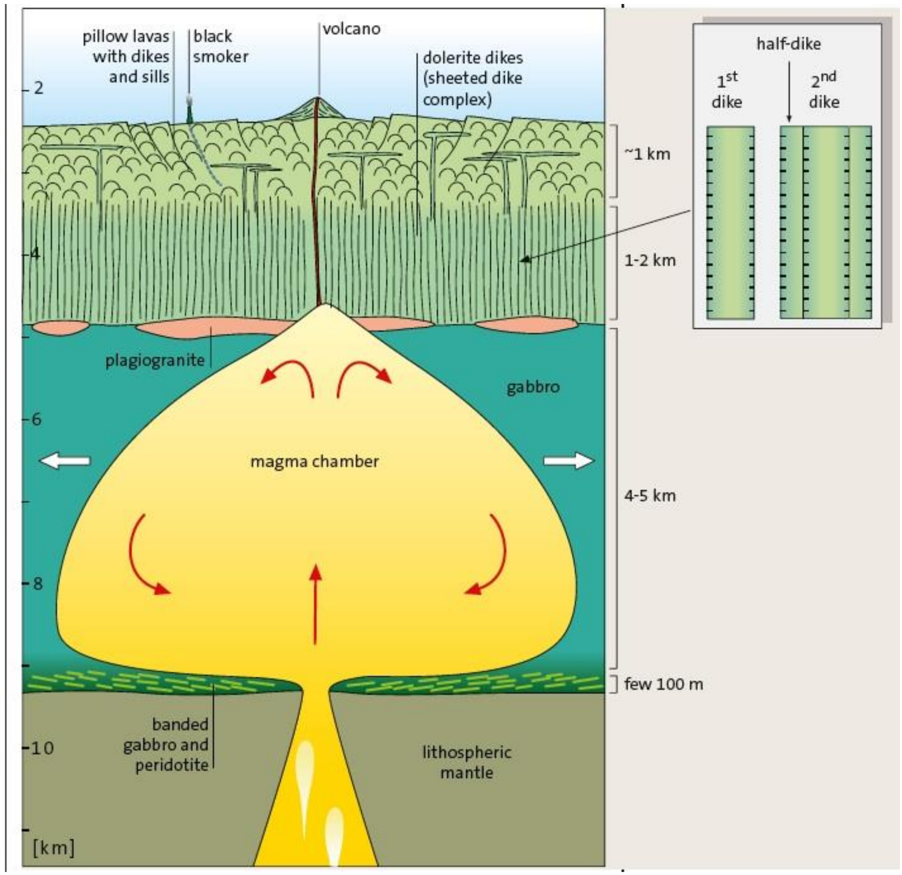

- Ridges have higher topography than the oceanic basins, being basaltic melts 15 % less dense than the peridotite.
- Mass surplus revealed by the gravity anomaly is related to the push up pressure caused by the rising of the asthenosphere.

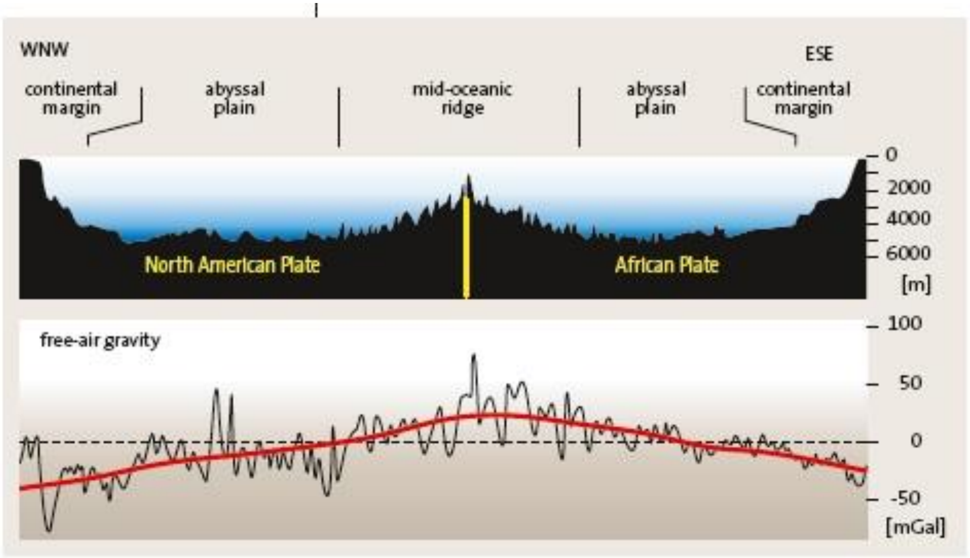

Continous basaltic melt extraction from the original lherzolite results in a harzburgite (olivine + enstatite)

$$lherzolite = harzburgite + basalt,$$

Mid-Ocean Ridges, petrology, topography, and gravity anomalies

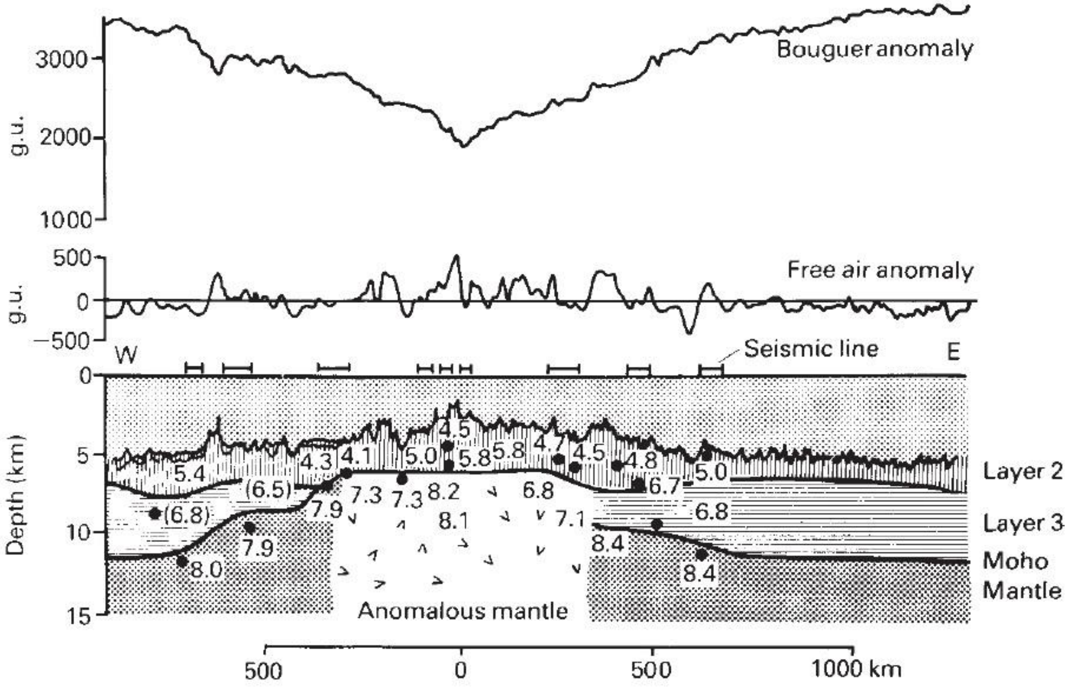

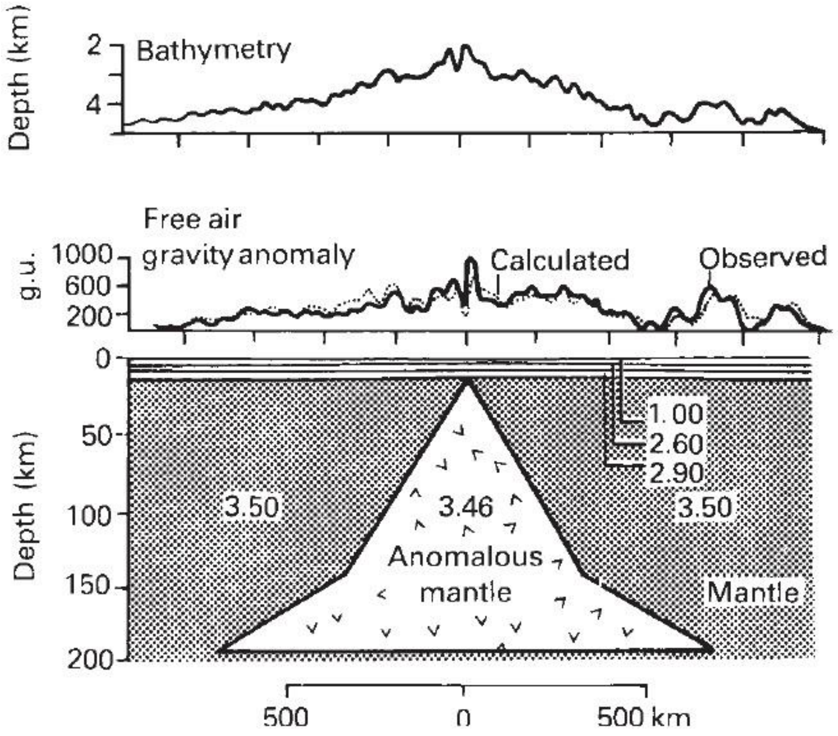

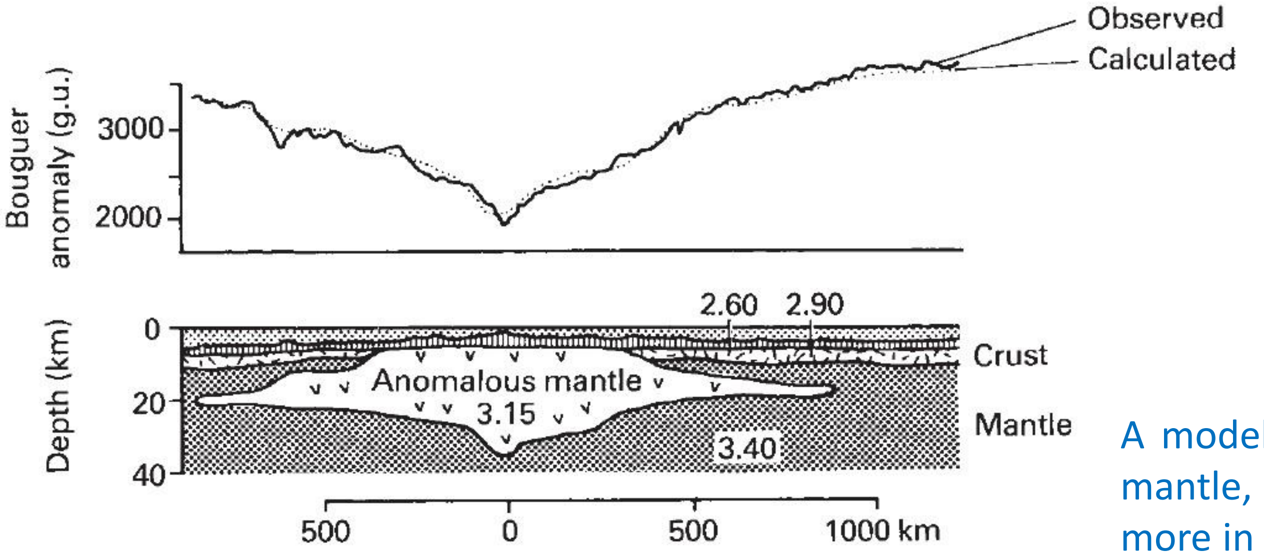

Low-density regions which underlie ocean ridges and support them isostatically may be related to:

(i) Thermal expansion of upper mantle material beneath the ridge crests, followed by contraction as sea floor spreading carries it laterally away from the source of heat.

(ii) The presence of molten material within the anomalous mantle,

(iii) Temperature-dependent phase change.

A model with densities of 3.35 and 3.28 g cm^{-3} for normal and anomalous mantle, with the anomalous mass extending to a depth of 100 km, would be more in agreement with geologic and geophysical data.

Marine magnetic anomalies

Magnetic lineations either side of the mid-Atlantic ridge south of Iceland

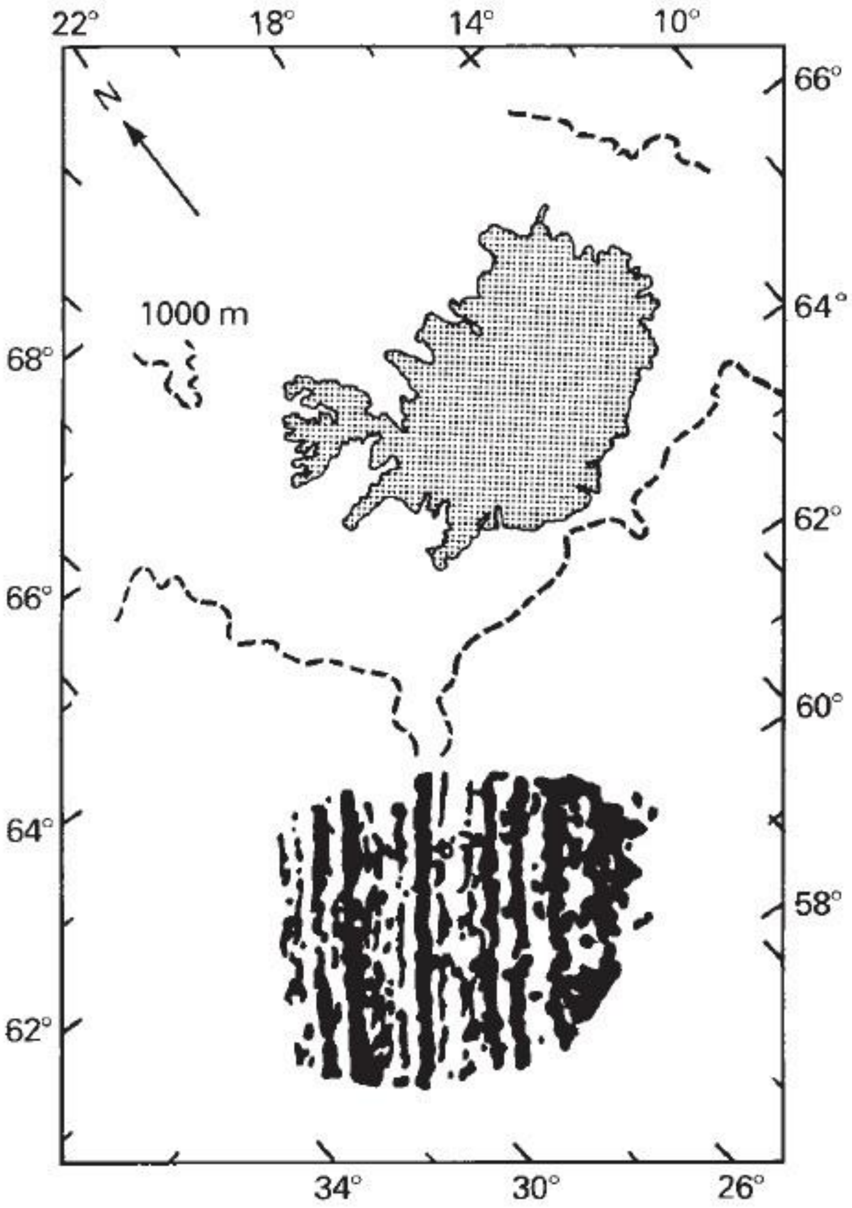

- Magnetic lineations are generally 10–20 km wide and characterized by a peak to peak amplitude of 500–1000 nT and present in all oceanic areas. They run parallel to the crests of the mid-ocean ridge system and are symmetrical about the ridge axes.
- Since the Earth magnetic field invert the polarity during the geological time, a ridge crest can be viewed as a twin-headed tape recorder in which the reversal history of the Earth’s magnetic field is registered within oceanic crust.
- The source of the magnetic anomalies is at least in part in oceanic layer 2, since basalt is known to contain a relatively high proportion of magnetic minerals.
- The shape of a magnetic anomaly is determined by both the geometric form of the source and the orientation of its magnetization vector: the lineations arise because adjacent blocks of layer 2 are magnetized in different directions.

Marine magnetic anomalies

- Blocks of normally magnetized crust formed at high northern latitudes possess a magnetization vector that dips steeply to the north (crust will be characterized by positive anomalies), and the vector of reversely magnetized material is inclined steeply upwards towards the south (crust will be characterized by negative anomalies).
- Crust magnetized at low latitudes also generates positive and negative anomalies in this way, but because of the relatively shallow inclination of the magnetization vector the anomaly over any particular block is markedly dipolar, with both positive and negative components (individual crustal blocks are no longer associated with a single positive or negative anomaly).
- At the magnetic equator, where the field is horizontal, negative anomalies coincide with normally magnetized blocks and positive anomalies with reversely magnetized blocks (the reverse situation to that at high latitudes).
- The amplitude of the anomaly decreases from the poles to the equator as the geomagnetic field strength, and hence the magnitude of the remanence decreases in this direction.

Variation of the magnetic anomaly pattern with geomagnetic latitude

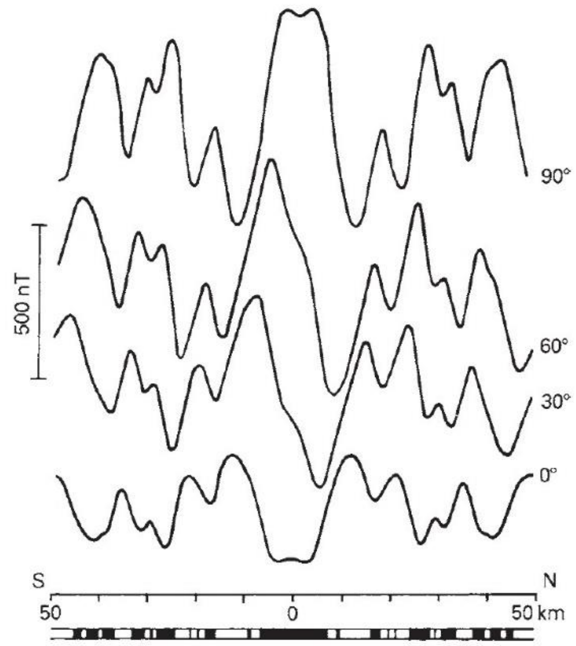

Variation of the magnetic anomaly pattern with the direction of the profile at a fixed latitude

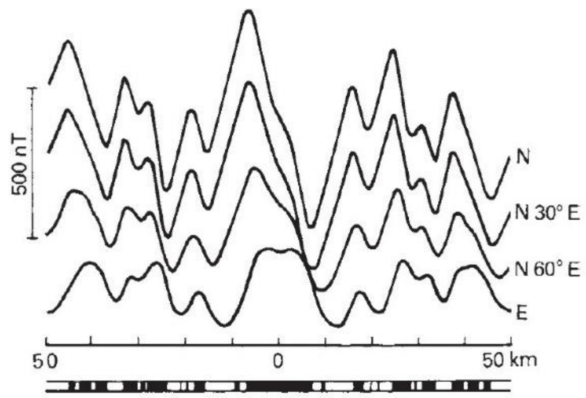

- Only the component of the magnetization vector lying in the vertical plane through the magnetic profile affects the magnetic anomaly.
- This component is at a maximum when the ridge is east-west and the profile north-south, and at a minimum for ridges oriented north-south.
- In general, the amplitude of magnetic anomalies decreases as the latitude decreases and as the strike of the ridge progresses from east-west to north-south.

Magnetostratigraphy

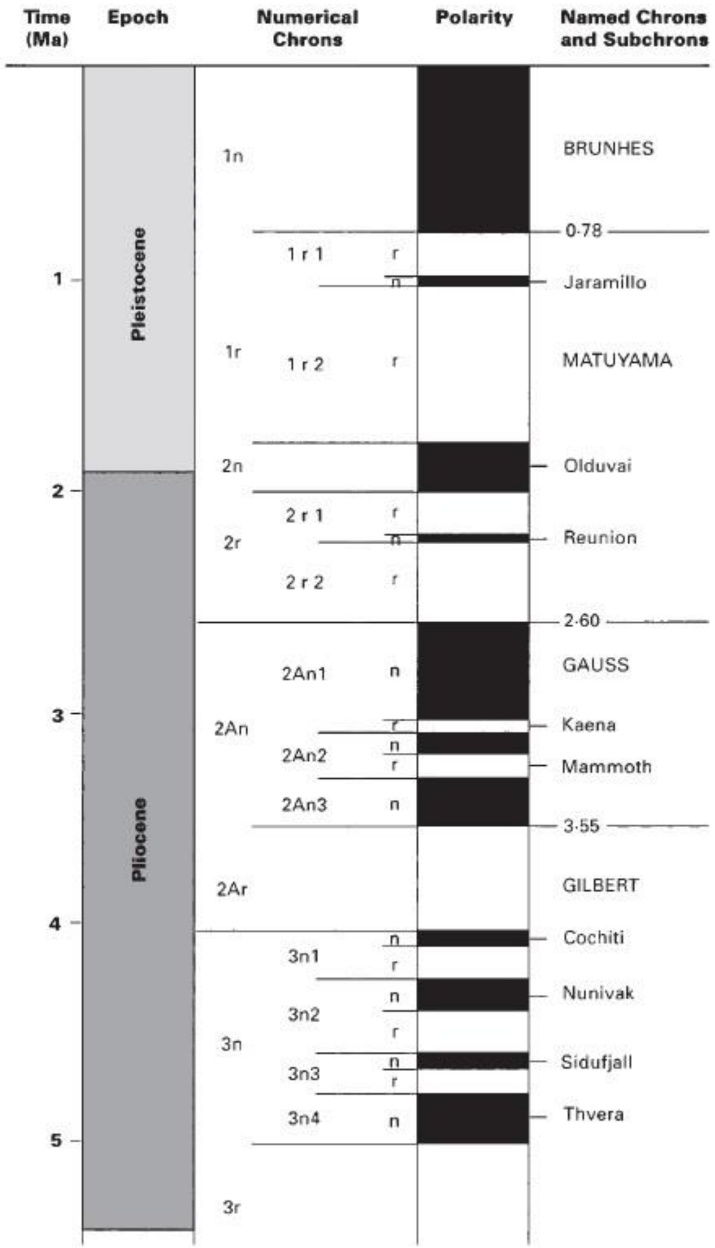

- Once the geomagnetic reversal timescale has been calibrated, oceanic magnetic anomalies may be used to date oceanic lithosphere back to Jurassic.
- The timescale to 5 Myr before present have been refined using K-Ar method, but polarity events of less than 50,000 years duration could not be resolved.
- Polarity chrons are defined with durations of the order of 10^6 years. Chrons may be dominantly of reversed or normal polarity, or contain mixed events.

By assuming a constant spreading rate in the South Atlantic it is possible to plot the distances to various magnetic anomalies from ridge crests in other oceans against the distance to the same anomalies in the South Atlantic:
Inflection points in the curves for the other oceans show when the spreading rates changed there.

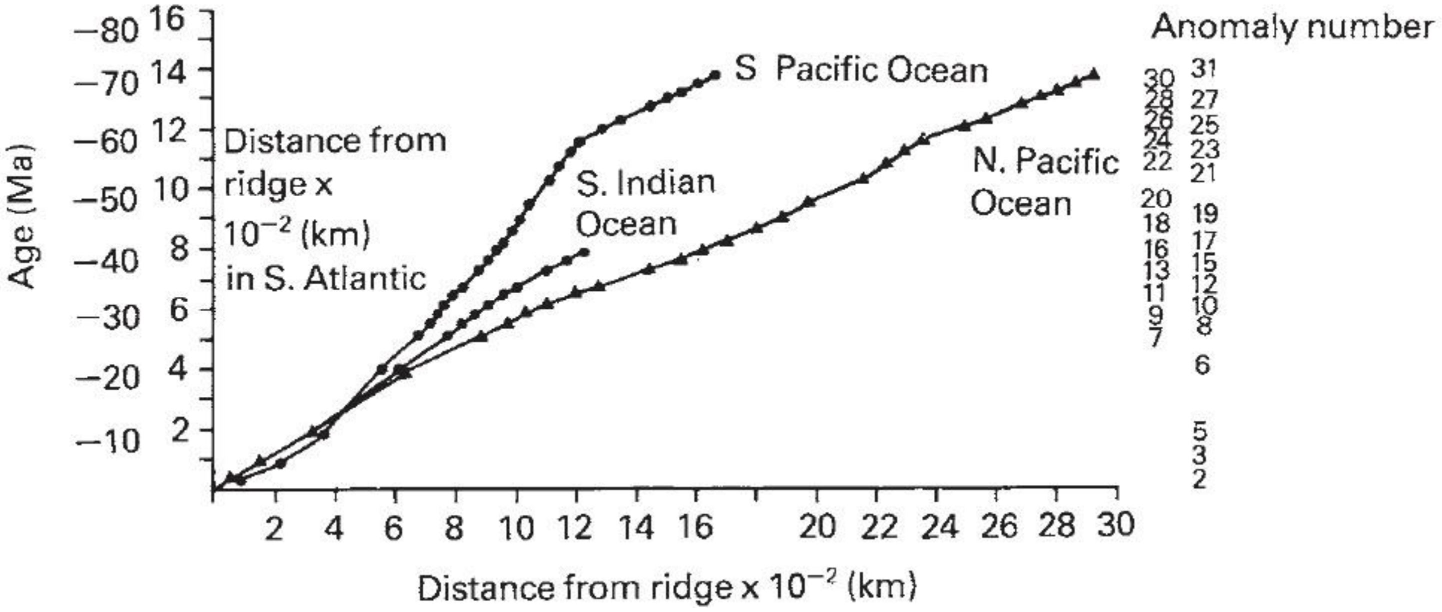

Dating the ocean floor

Relationship between greatest sediment age and distance from the Mid-Atlantic Ridge crest

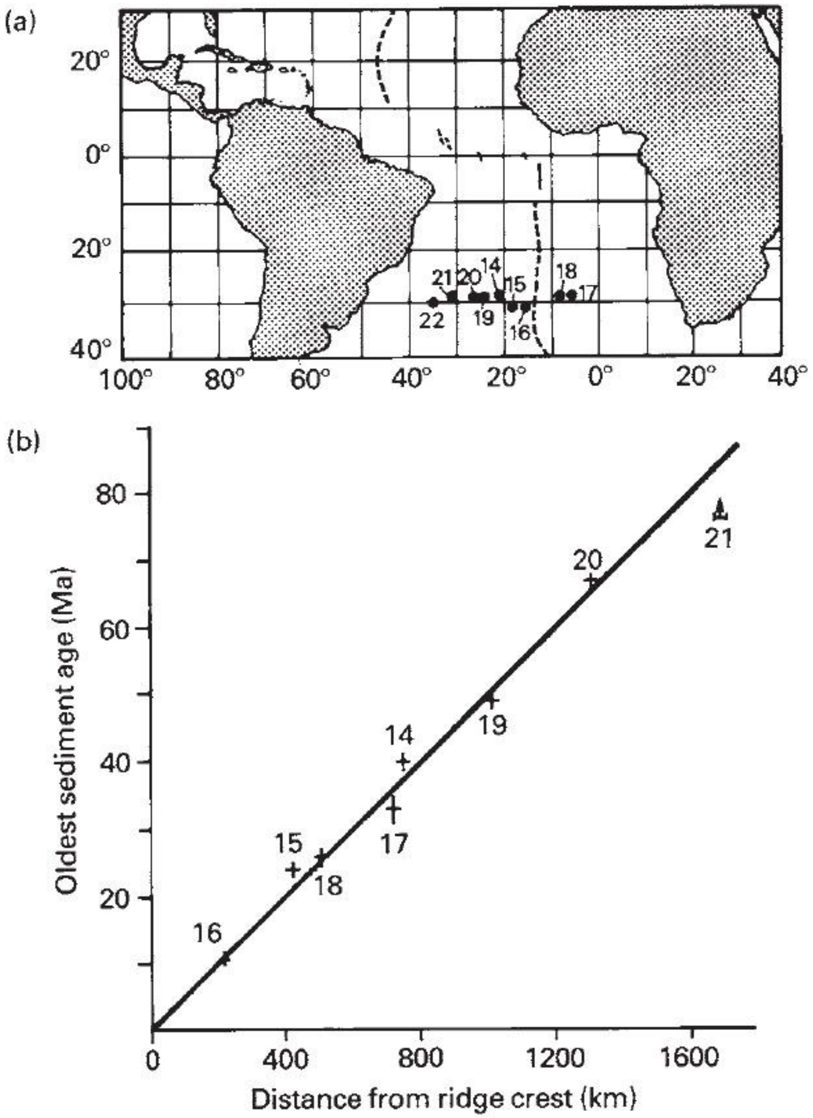

- The crustal age in the South Atlantic is estimated plotting the age of the sediments vs distance from the ridge. The predicted ages imply a half spreading rate in this region of 20 mm yr^{-1}.
- The use of the geomagnetic timescale to date the oceanic lithosphere is based on the identification of characteristic patterns of magnetic anomaly lineations and their relation to the dated reversal chronology.
- Once the reversal chronology has been established, lineations of known age can be identified on magnetic maps and transformed into isochrones, so that the sea floor can be subdivided into age provinces.

Age and thickness of oceanic lithosphere (observations)

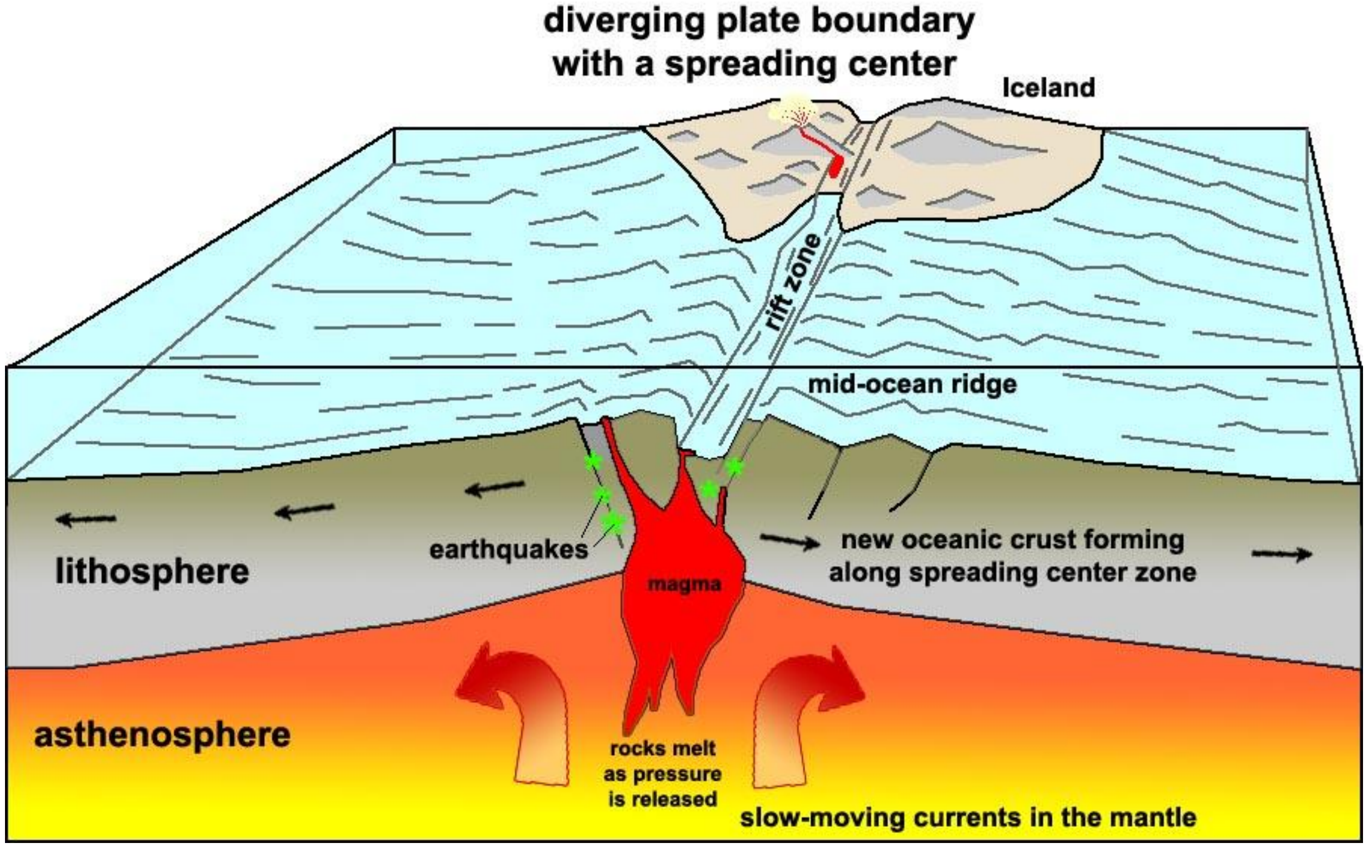

Cooling causes a progressive increase in the density and thickness of the lithosphere
(e.g., In the Pacific Ocean lithospheric thickness is 30 km after 5myr and about 100 km after 50 Myr)

Age and Temperature of Oceanic Lithosphere

Oceanic Age

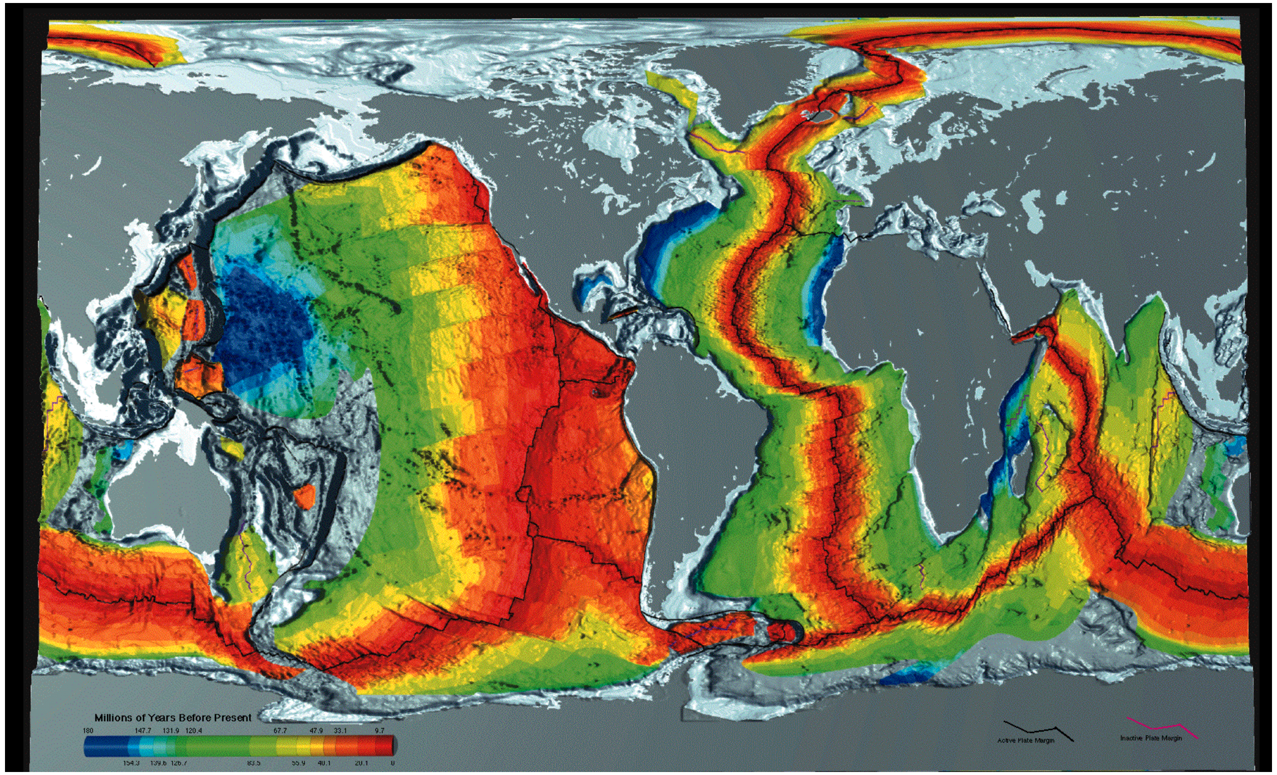

Oceanic Surface Heat Flow

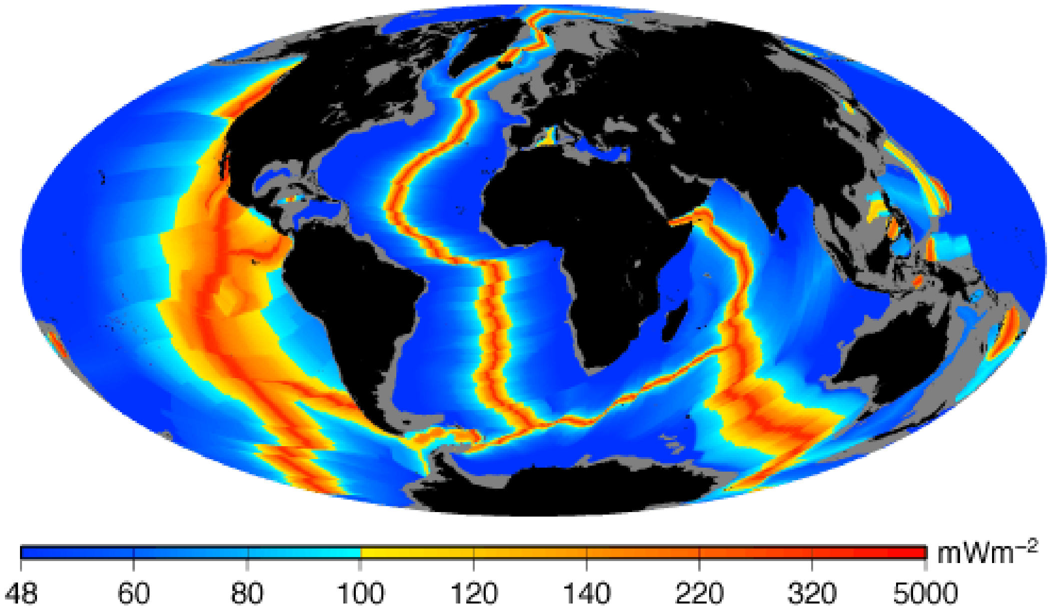

Oceanic average HF: 67 mWm^2 (only due to conduction), 101 mWm^{-2} (including heat loss form hot fluids)

Unified Thermal Boundary Layer Model

- Plate dynamics is governed by a thermomechanical boundary layer that evolves by conductive decay

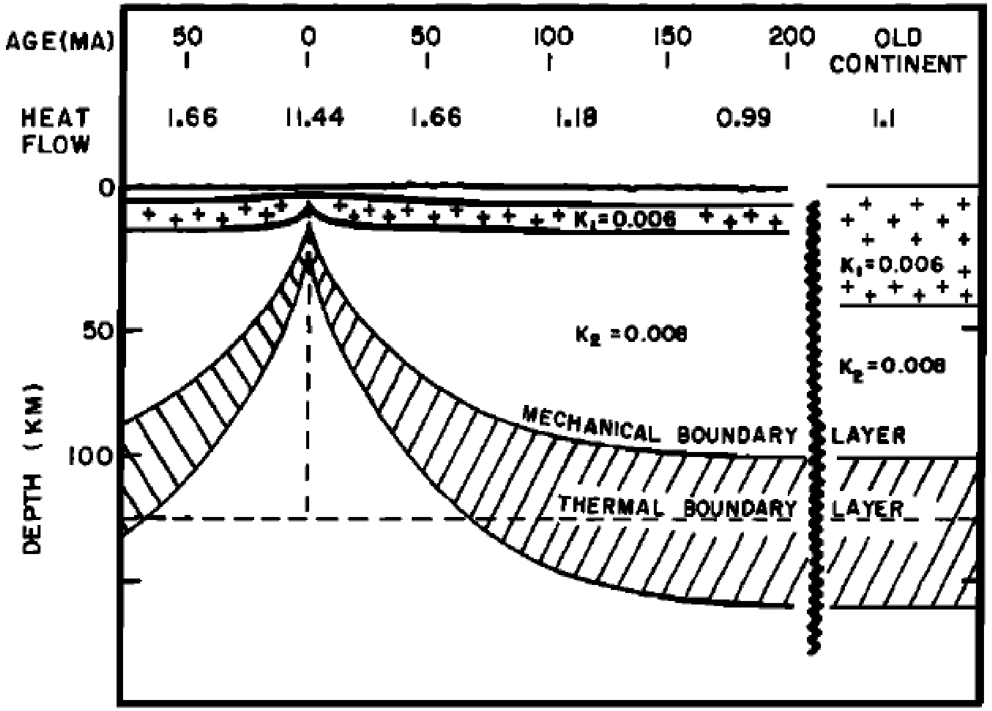

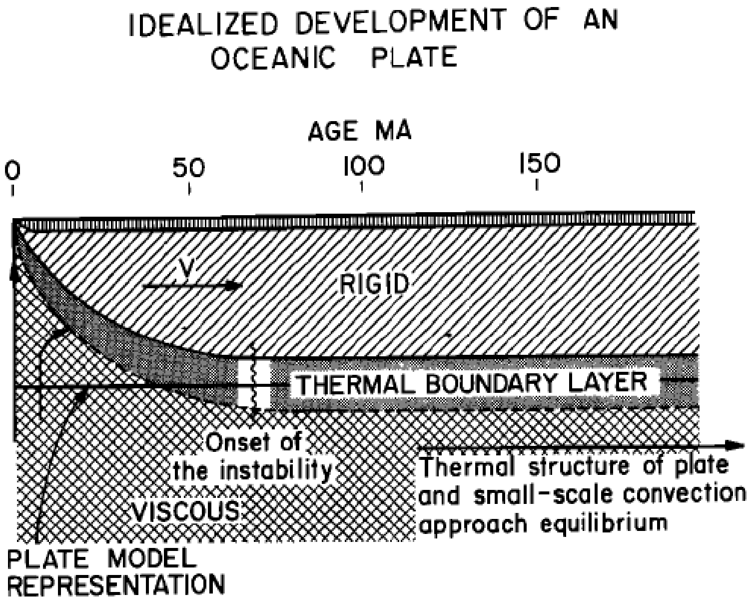

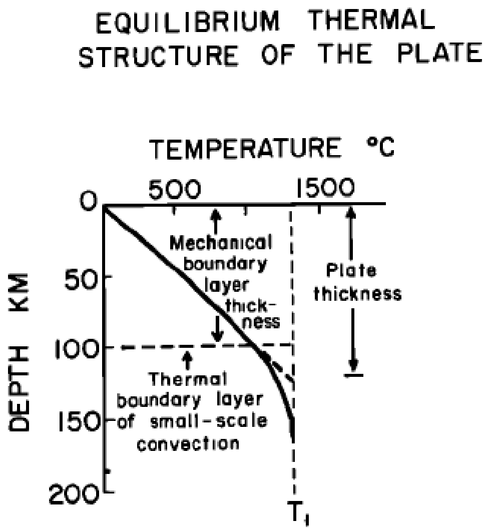

TBL thickness maintained by convective instability

Sclater et al. (1981), after Parsons & McKenzie (1978)

Cooling models for oceanic heat flux

The cooling model predicts how heat flux decreases and how the depth of the sea floor increases with age of the sea floor

- In the oceanic realm, flow is dominantely horizontal, but the large wavelengths of Q variations imply a predominant vertical heat transfer. If x is the distance from the ridge and z the depth from the sea floor, temperature equation is:

$$\rho C_p\left(\frac{\partial T}{\partial t}+u\frac{\partial T}{\partial x}\right)=\frac{\partial}{\partial z}\left(\lambda\frac{\partial T}{\partial z}\right)$$

$\frac{\partial}{\partial z}\left(\lambda\frac{\partial T}{\partial z}\right)$ = advection of heat with moving plate

u = horizontal velocity, ρ = density of the lithosphere, C_p= heat capacity , λ=thermal conductivity

In steady state conditions, for a constat λ:

$$\rho C_p u\frac{\partial T}{\partial x}=\lambda\frac{\partial^2 T}{\partial z^2}$$

For a constant spreading rate, the age τ is:

$$\tau = x/u \qquad\qquad \frac{\partial T}{\partial \tau}=\kappa\frac{\partial^2 T}{\partial z^2}$$

z=depth (m)
$\kappa=\lambda/\rho C_p$=thermal diffusivity (10^{-6} m^2s^{-1} or 31.5 km^2 Myr^{-1})

Error Function (erf(x))

In mathematics, the **error function** (also called the **Gauss error function**) is a special function (non-elementary) of sigmoid shape that occurs in probability, statistics, and partial differential equations:

$$\operatorname{erf}(x) := \frac{2}{\sqrt{\pi}} \int_0^x e^{-t^2}\, dt\,.$$

$$\operatorname{erfc}(x) := 1 - \operatorname{erf}(x) = \frac{2}{\sqrt{\pi}} \int_x^\infty e^{-t^2}\, dt$$

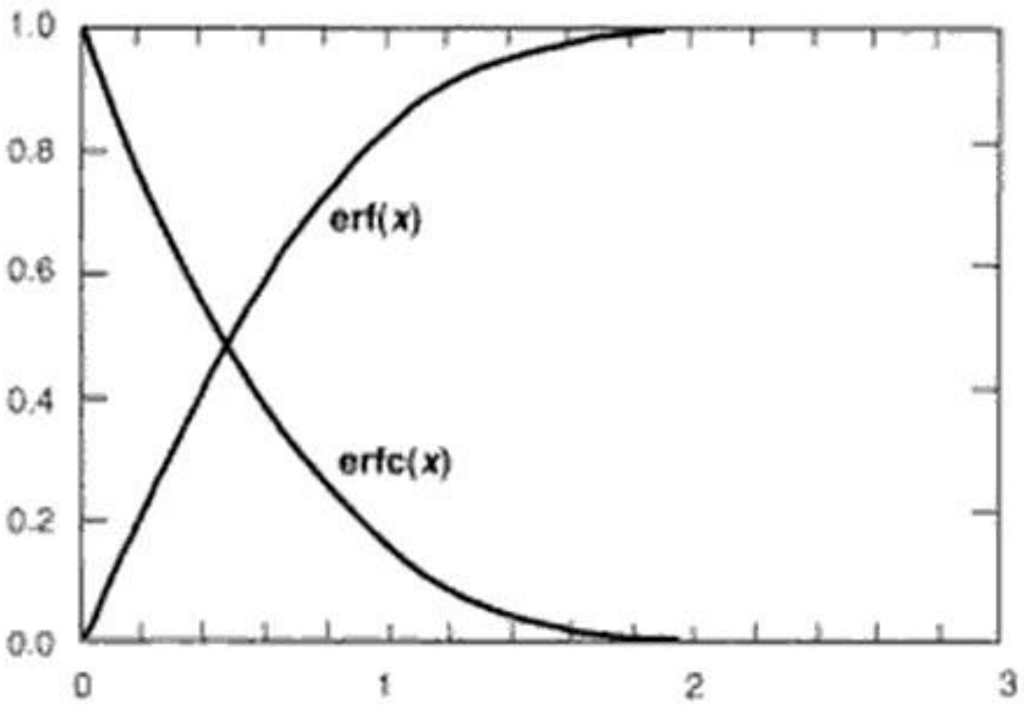

x	erf(x)	erfc(x)	x	erf(x)	erfc(x)
0,00	0,0000000	1,0000000	1,30	0,9340079	0,0659921
0,05	0,0563720	0,9436280	1,40	0,9522851	0,0477149
0,10	0,1124629	0,8875371	1,50	0,9661051	0,0338949
0,15	0,1679960	0,8320040	1,60	0,9763484	0,0236516
0,20	0,2227026	0,7772974	1,70	0,9837905	0,0162095
0,25	0,2763264	0,7236736	1,80	0,9890905	0,0109095
0,30	0,3286268	0,6713732	1,90	0,9927904	0,0072096
0,35	0,3793821	0,6206179	2,00	0,9953223	0,0046777
0,40	0,4283924	0,5716076	2,10	0,9970205	0,0029795
0,45	0,4754817	0,5245183	2,20	0,9981372	0,0018628
0,50	0,5204999	0,4795001	2,30	0,9988568	0,0011432
0,55	0,5633234	0,4366766	2,40	0,9993115	0,0006885
0,60	0,6038561	0,3961439	2,50	0,9995930	0,0004070
0,65	0,6420293	0,3579707	2,60	0,9997640	0,0002360
0,70	0,6778012	0,3221988	2,70	0,9998657	0,0001343
0,75	0,7111556	0,2888444	2,80	0,9999250	0,0000750
0,80	0,7421010	0,2578990	2,90	0,9999589	0,0000411
0,85	0,7706681	0,2293319	3,0	0,9999779	0,0000221
0,90	0,7969082	0,2030918	3,10	0,9999884	0,0000116
0,95	0,8208908	0,1791092	3,20	0,9999940	0,0000060
1,00	0,8427008	0,1572992	3,30	0,9999969	0,0000031
1,10	0,8802051	0,1197949	3,40	0,9999985	0,0000015
1,20	0,9103140	0,0896860	3,50	0,9999993	0,0000007

$$\operatorname{erf}(x) = \frac{2}{\sqrt{\pi}} \sum_{n=0}^{\infty} \frac{(-1)^n x^{2n+1}}{(2n+1)n!} = \frac{2}{\sqrt{\pi}} \left(x - \frac{x^3}{3} + \frac{x^5}{10} - \frac{x^7}{42} + \frac{x^9}{216} - \cdots \right)$$

Half-space (*HS*) cooling model

Assuming that the mantle is a uniform infinite halfspace, with the initial condition that *T(z,* 0) = *Tm*, the boundary condition that *T(0, t)* = 0 and the assumption that radioactive heating can be neglected:

$$T(z,t) = T_{\mathrm{m}}\mathrm{erf}\left(\frac{z}{2\sqrt{\kappa t}}\right)$$

or we can write in the form:

$$T(z,\tau) = \Delta T \mathrm{erf}\left(\frac{z}{2\sqrt{\kappa\tau}}\right) = \frac{2\Delta T}{\sqrt{\pi}}\int_0^{z/2\sqrt{\kappa\tau}} \exp(-\eta^2)d\eta$$

$$x = z/2\sqrt{(\kappa t)}$$

$$\frac{\mathrm{d}\,\mathrm{erf}(x)}{\mathrm{d}x} = \mathrm{erf}'(x) = \frac{2}{\sqrt{\pi}}\mathrm{e}^{-x^2}$$

$$\frac{\partial T}{\partial z} = T_{\mathrm{m}}\frac{\mathrm{d}\,\mathrm{erf}(x)}{\mathrm{d}x}\frac{\partial x}{\partial z} = T_{\mathrm{m}}\frac{2}{\sqrt{\pi}}\mathrm{e}^{-x^2}\frac{1}{2\sqrt{\kappa t}}$$

The heat flux q_0 at z = 0 is

$$q_0 = -K\left.\frac{\partial T}{\partial z}\right|_{z=0} = -\frac{KT_{\mathrm{m}}}{\sqrt{\pi\kappa t}}$$

λ=*K*=thermal conductivity

Half-space (*HS*) cooling model

In the half-space mode, the depth of isotherms increases with age, or distance form the spreading center

$$q(\tau) = \lambda \frac{\Delta T}{\sqrt{\pi \kappa \tau}} = C_Q \tau^{-1/2} \qquad C_Q = \lambda \Delta T / \sqrt{\pi \kappa}$$

C_Q=*HF* cooling constant

- The heat flux values can be fitted by a $\tau^{-1/2}$ relationship with the constant C_Q between 470 and 510 mW m^{-2} My$^{1/2}$.
- Heat flux data selected from sites where thick sedimentary cover is hydraulically resistive and seals off hydrothermal circulation fit the *HS* cooling model, with the constraint that for HF $\longrightarrow$0 as age$\longrightarrow\infty$ and excluding ocean floor > 80Myr.

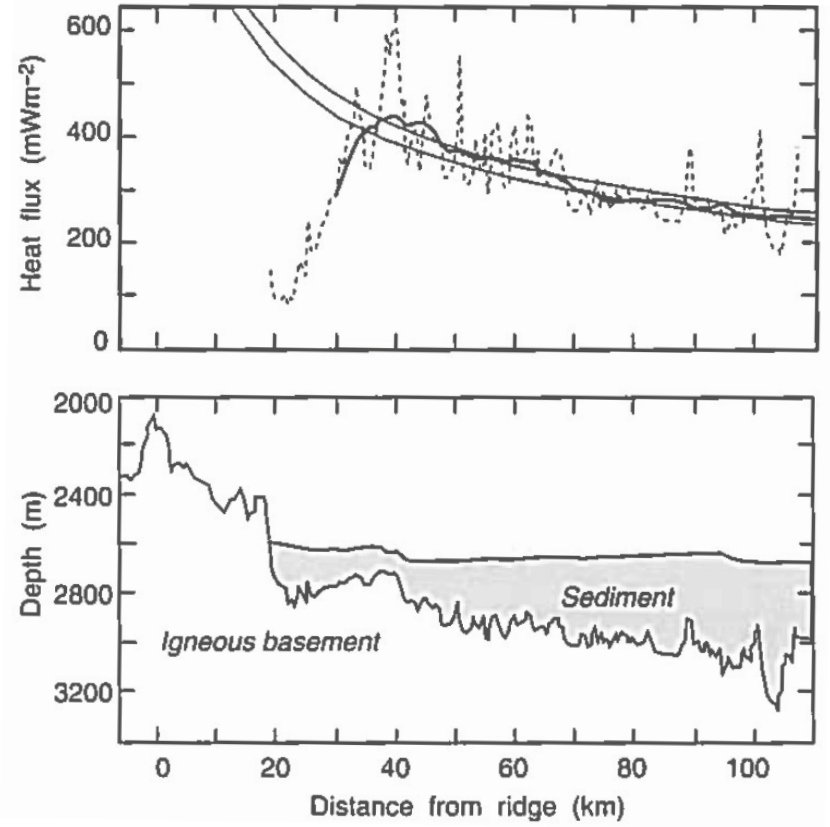

Depth of the isotherms as a function of sea-floor age *t*

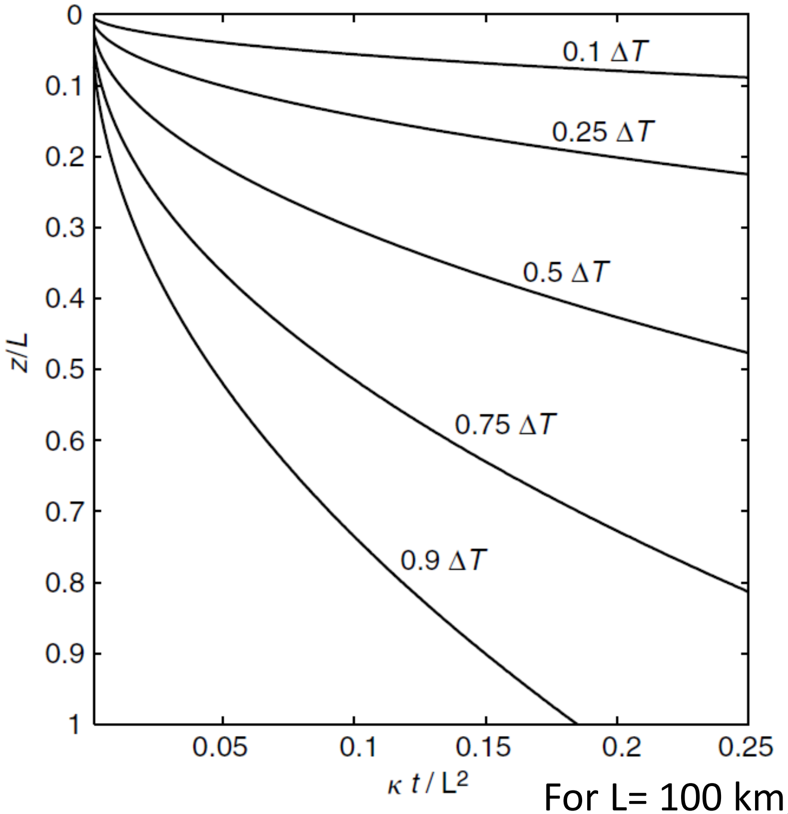

For L= 100 km, t = 0.25 L^2/κ= 80 Myr

Half-space (HS) cooling model

Oceanic lithospheric thickness increases with age: $h = \sqrt{\pi \kappa \tau}$

- **Due to hydrothermal circulation, heat flux data close to the ridges are very scatterred**
- The heat loss by hydrothermal circulation (~ 11 TW) can be obtained as the difference between the predicted *HF* (*HS* cooling model) and the average measured *HF* within each age bin (~ 550 mWm^{-2}) and integrating this difference over the entire sea floor.

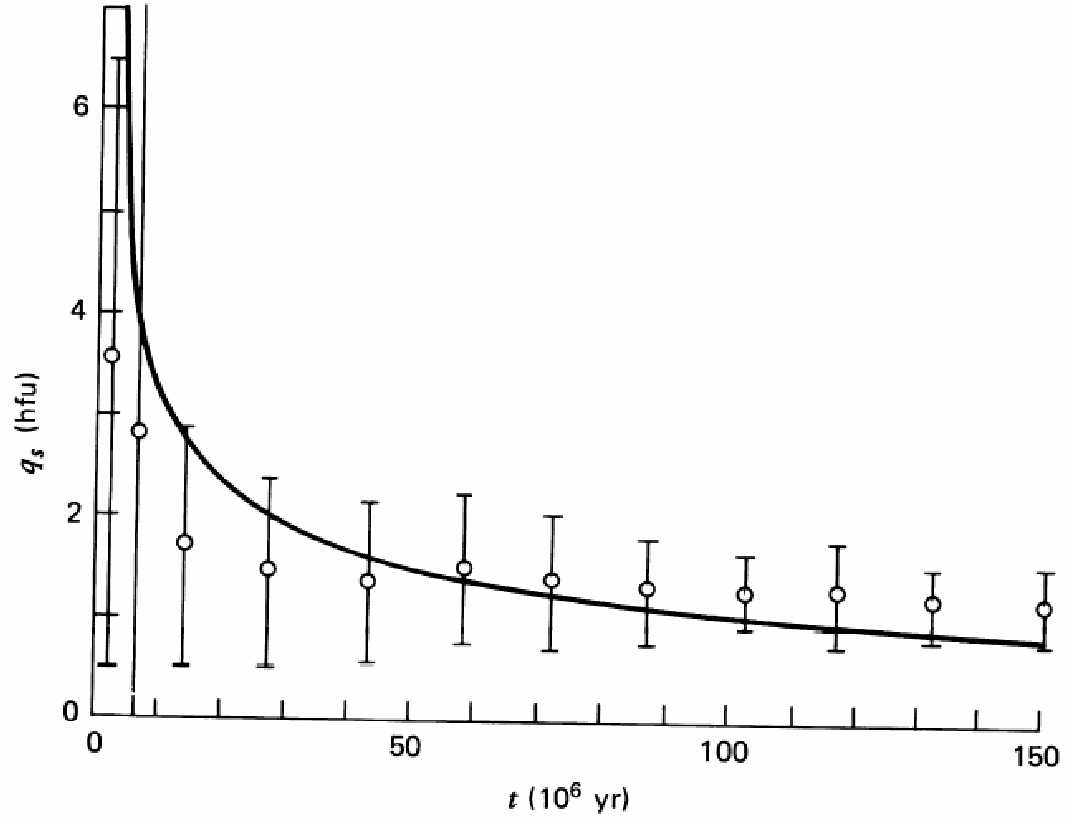

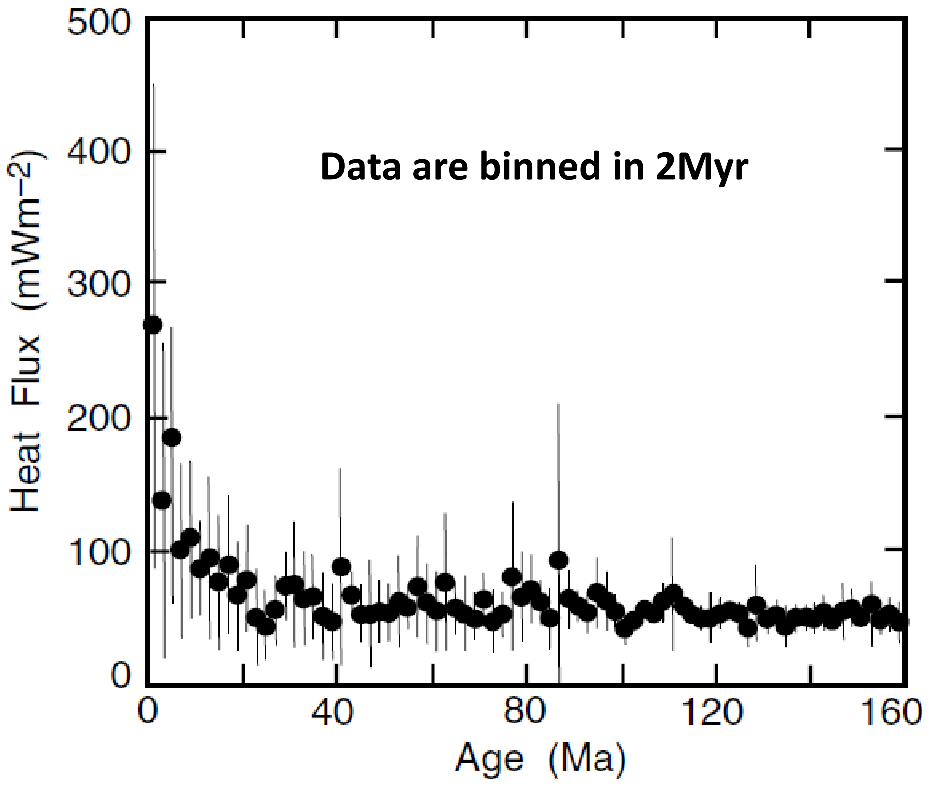

Half-space (HS) cooling model

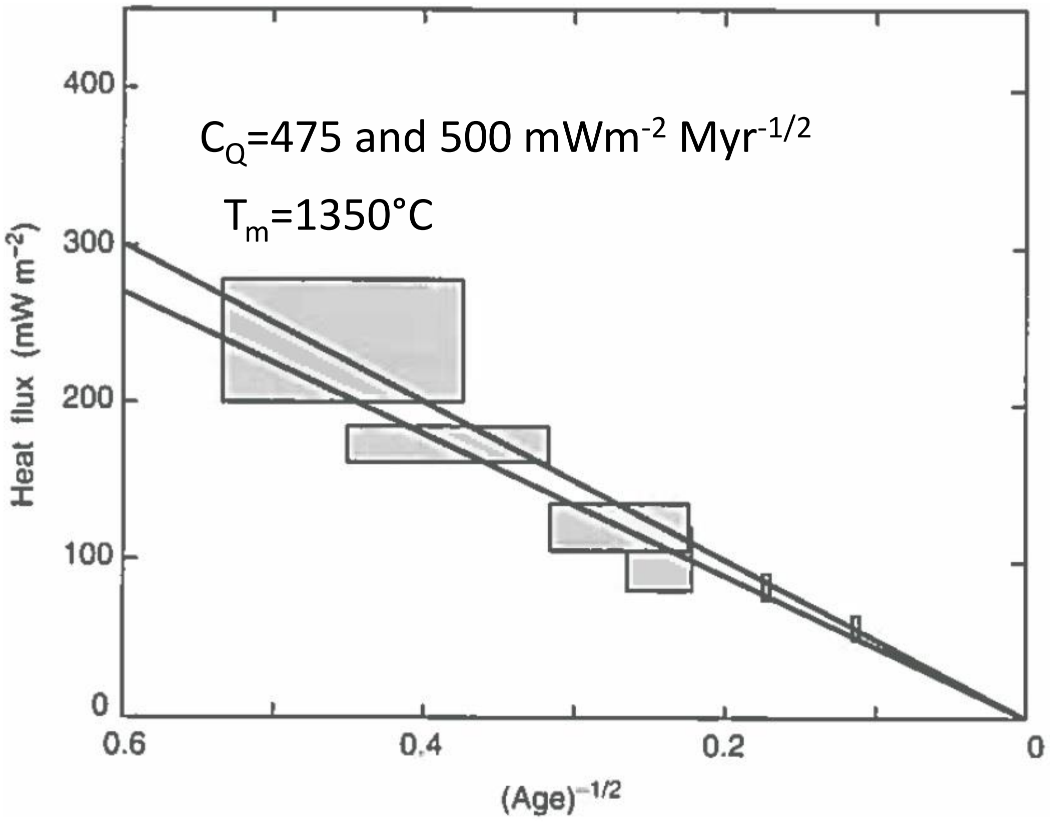

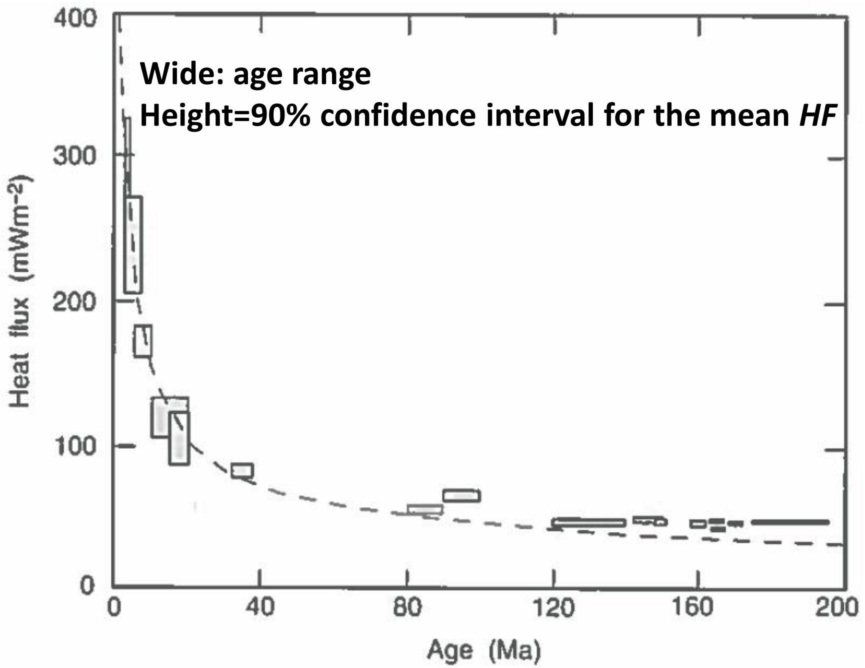

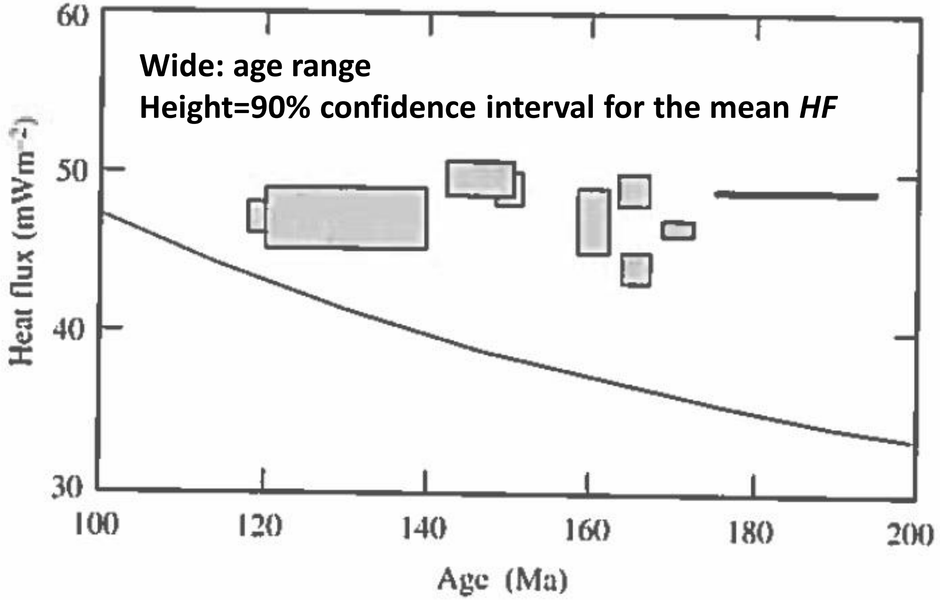

- **Heat flux data through sea floor > 80 Myr are sistematically higher than model prediction.**

Half-space (HS) cooling model

- Bathymetry records the total cooling of the oceanic lithosphere since its formation at the mid-oceanic ridges and are far less noisy than heat flux data.
- Bathymetry fits extremely well the predictions of the *HS* cooling model for oceanic lithosphere younger than ≈100 My.
- However, flattening of the bathymetry does not allow straightforward conclusions (depth values exhibit some scatter due to inaccurate estimates of sediment thickness, presence of sea-mounts, and large hot spot volcanic edifices).

After a correction for isostatic adjustments to sediment loading, the basement depth for oceanic age < 80 Myr:

$$h(\tau) = (2600 \pm 20) + (345 \pm 3)\tau^{1/2}$$

$$q(\tau) = (480 \pm 4)\tau^{-1/2}$$

h (m), τ (Myr), and *q*=mWm^{-2}

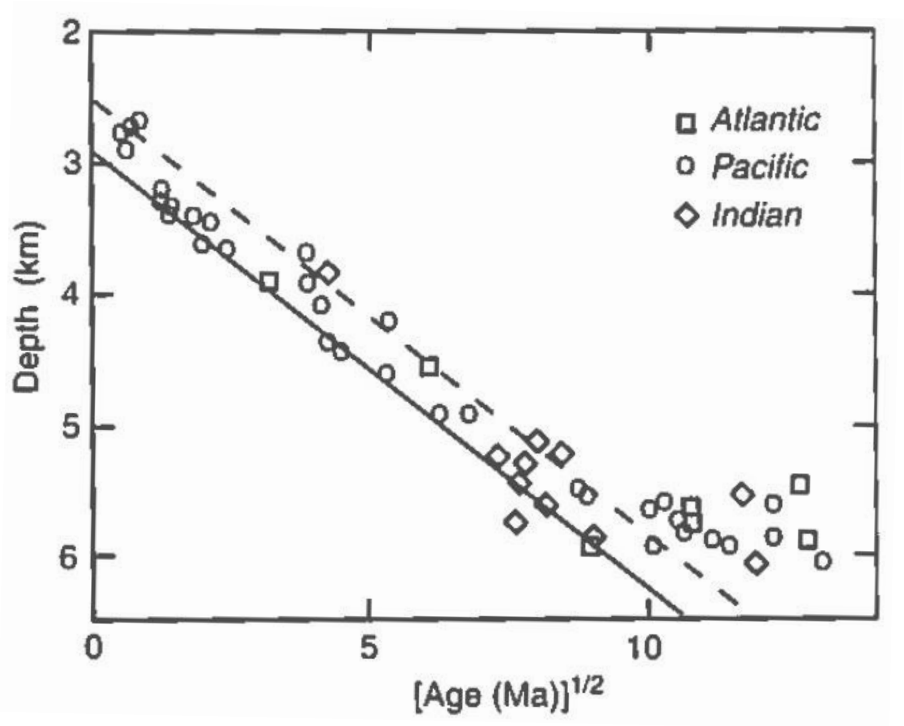

Depth of Earthquakes in the Oceans *vs* Age of the Sea Floor
(Isotherms for a HS cooling model)

Depth of the earthquakes as function of sea-floor age

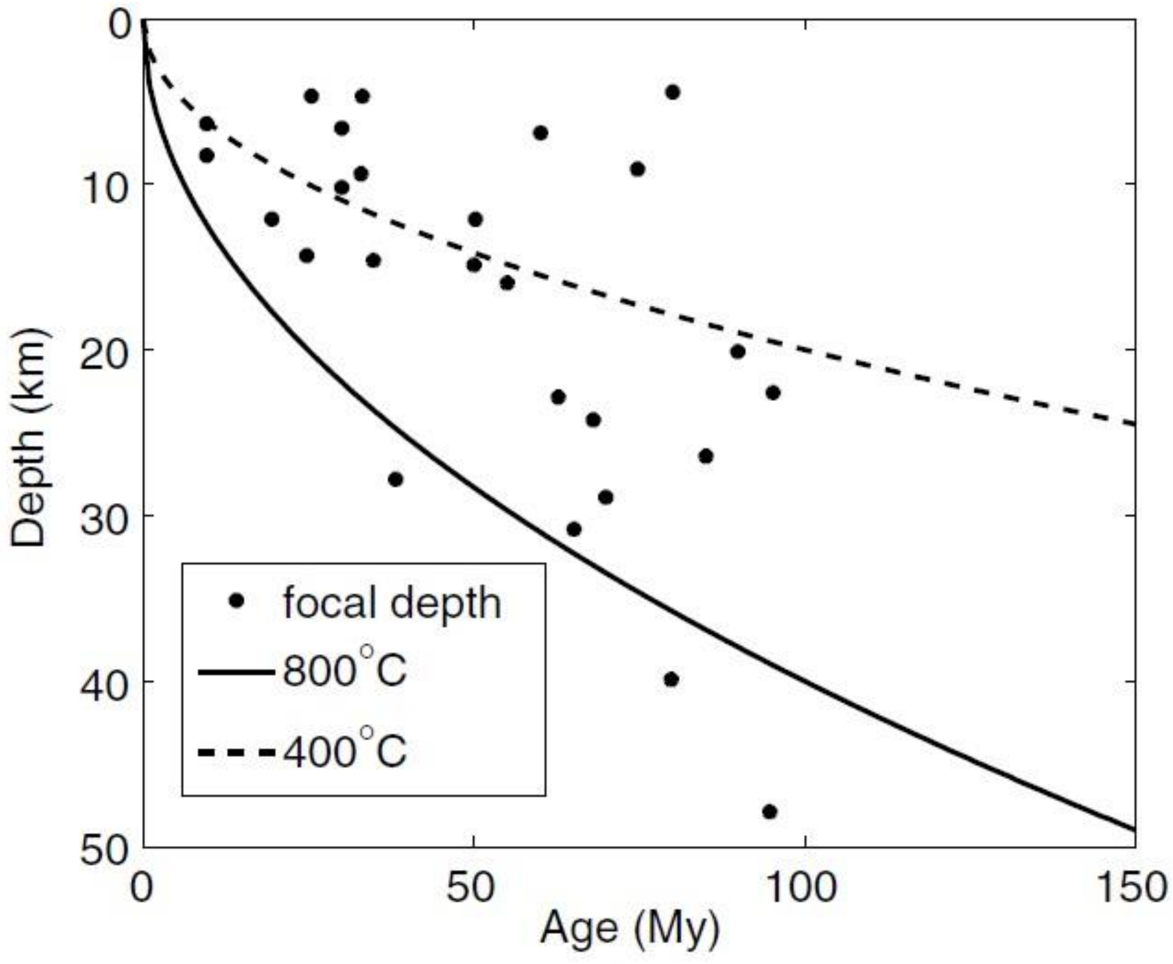

Effective Elastic Thickness as function of sea-floor age

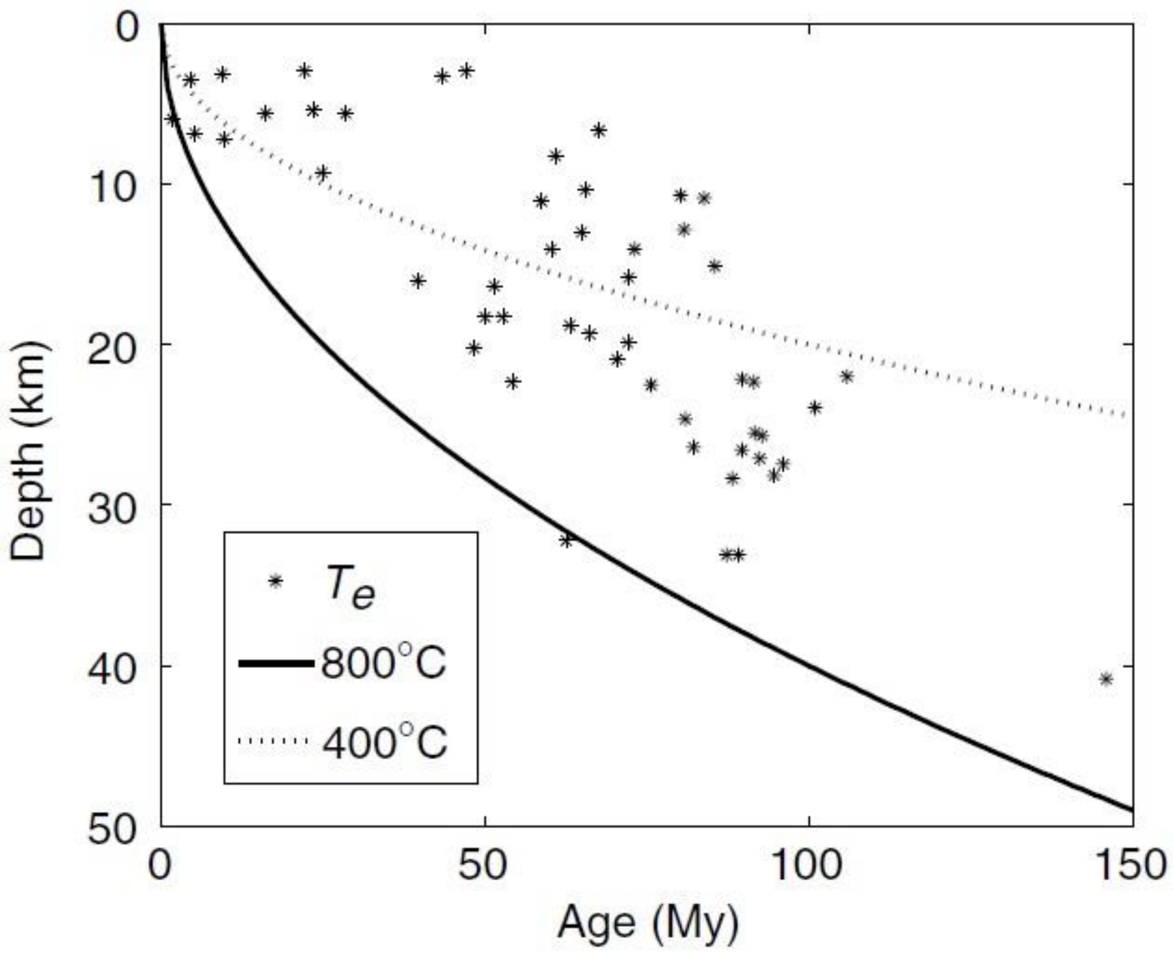

Why do we need a plate model?

- Heat flux data exhibit no detectable variation at ages >80-120My (q_0 levels off ~48 mWm^{-2}).
- Departure of heat flux data from the $1/\sqrt{\tau}$ behavior, indicates that heat is supplied to the lithosphere from below.
- Flattening of the bathymetry and heat flux implies that heat is brought into the lithosphere from below at the same rate as it is lost at the surface.
- Small scale convection occurs in the asthenosphere at the base of the old lithosphere, which would increase the *HF* into the base of the lithosphere and maintain a more constant lithospheric thickness.
- Then, we need a "plate" model for which a boundary condition is specified at some fixed depth (the base of the plate).

In the plate model the oceanic lithosphere is taken to be of constant thickness L and at its base T is equal to T_a (temperature of the asthenosphere) and at its top T=0.

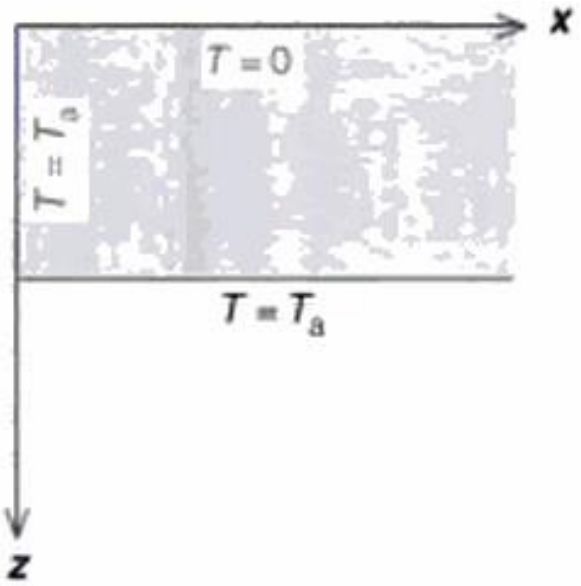

Plate Cooling Model
(with fixed temperature at the base)

The temperature within the plate (when the horizontal conduction of heat is neglected) is:

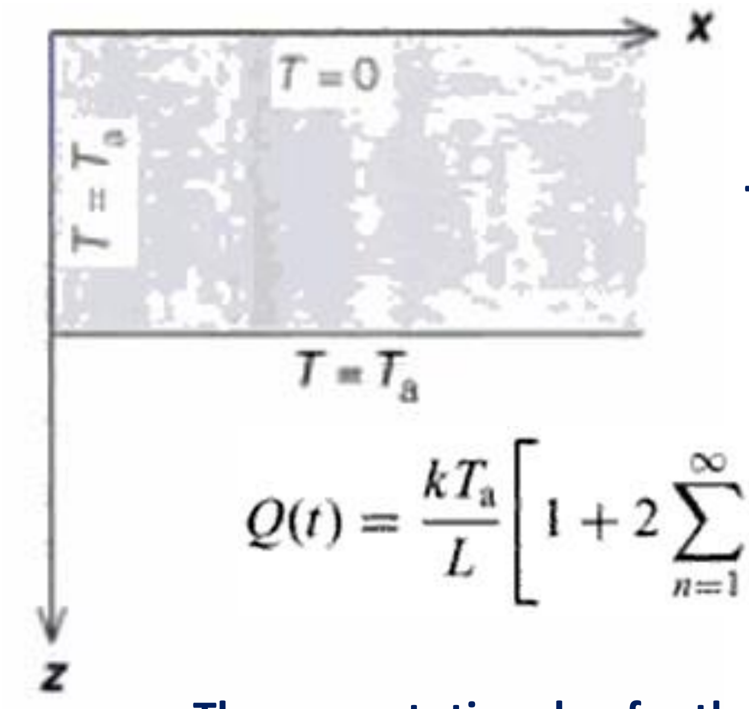

$$T = T_a\left[\frac{z}{L} + \sum_{n=1}^{\infty}\frac{2}{n\pi}\sin\left(\frac{n\pi z}{L}\right)\exp\left(-\frac{n^2\pi^2\kappa t}{L^2}\right)\right]$$

The characteristic time τ (relaxation time) is: $\tau = L^2/\kappa$

For t>>τ

$$T = T_a\left[\frac{z}{L} + \frac{2}{\pi}\sin\left(\frac{\pi z}{L}\right)\exp\left(-\frac{\pi^2\kappa t}{L^2}\right)\right]$$

$$Q(t) = \frac{kT_a}{L}\left[1 + 2\sum_{n=1}^{\infty}\exp\left(-\frac{n^2\pi^2 t}{L^2}\right)\right]$$

K or λ=thermal conductivity

$T_a = T_T$ $L = a_T$= Depth of the lithosphere

The asymptotic value for the heat flow is: $\frac{kT_a}{L}$ which can be written as: $\frac{\lambda\Delta T_T}{\sqrt{\pi\kappa t}}$

The depth of the lithosphere as a function of the age, d(t) is: $h(t) = \frac{\alpha\Delta T_T L}{2}\left(1 - \frac{8}{\pi^2}\sum_{n=1}^{\infty}\frac{1}{(2n-1)^2}\exp\left(\frac{-(2n-1)^2\pi^2\kappa t}{L^2}\right)\right)$

- **The plate cooling model has a uniformly thick lithosphere, then *T* of the lithosphere approaches the equilibrium as the age increases.**

$h(t) = \frac{\alpha\Delta T_T L}{2}$ **(asymptotic value for the depth of the lithosphere)**

Plate cooling model vs Half-Space cooling model

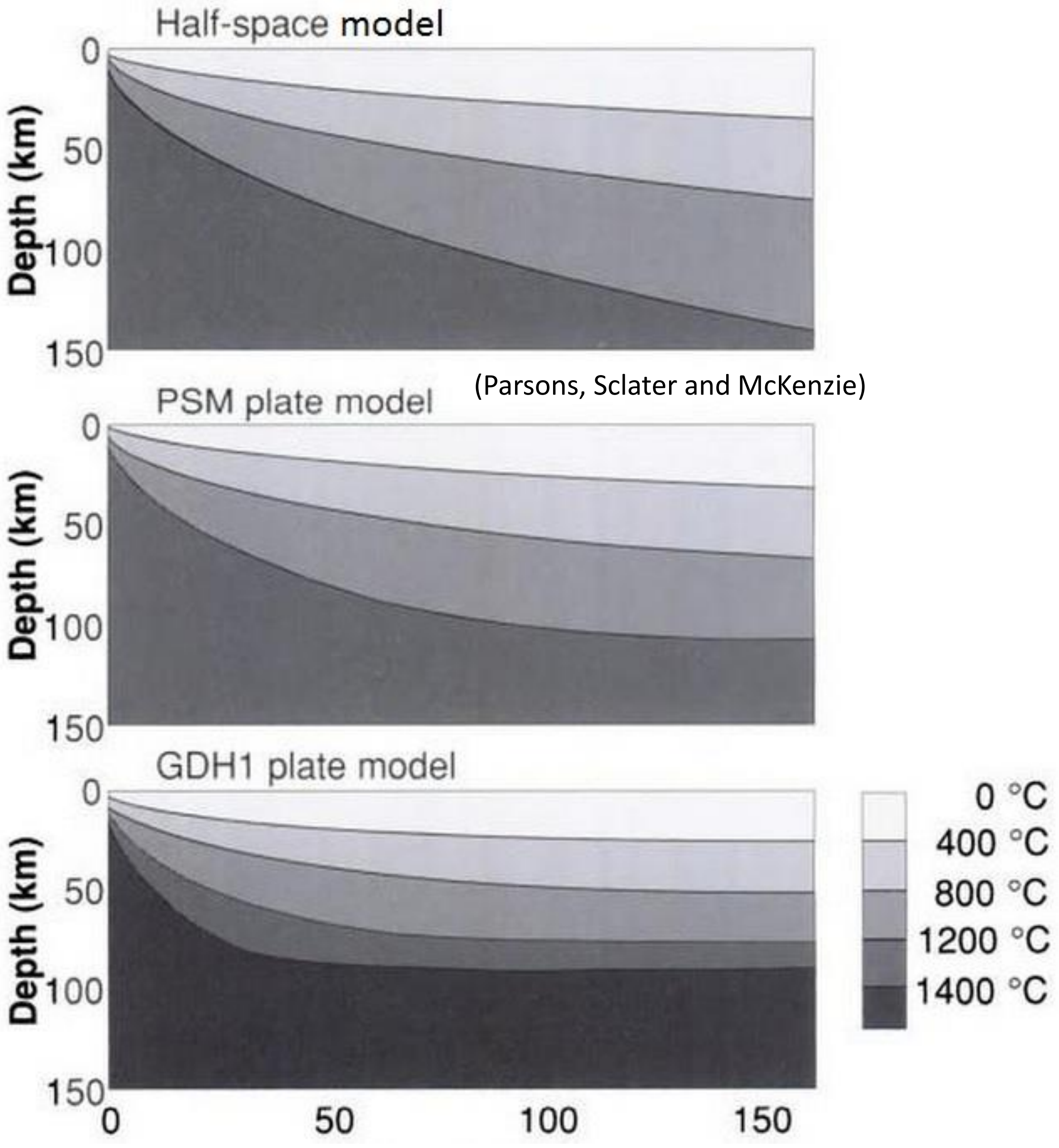

Depth and heat flow – observations

Which model(s) fit the data?

HS – Half-space model
GDH1 – plate model
PSM – plate model

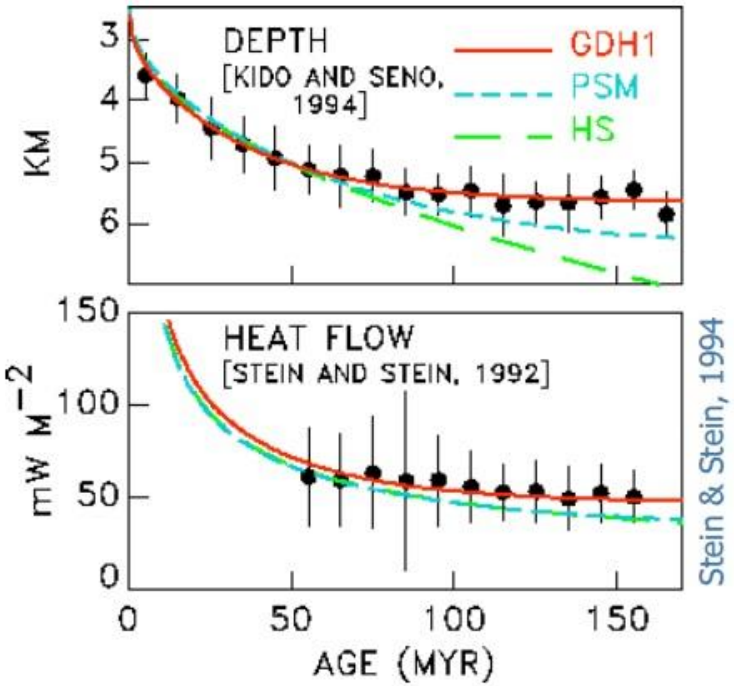

The GDH1 "plate" model does a better job of fitting the depth data
(which is better constrained)

All fit the heat flow data
(within error)

- **GDH1 has a thinner plate and higher temperatures than the other models**
- ***HS* cooling model fits the ocean-depth datasets for young lithosphere better than plate cooling model.**

Plate cooling model vs Half-Space cooling model

Depth and heat flow – observations

Which model(s) fit the data?

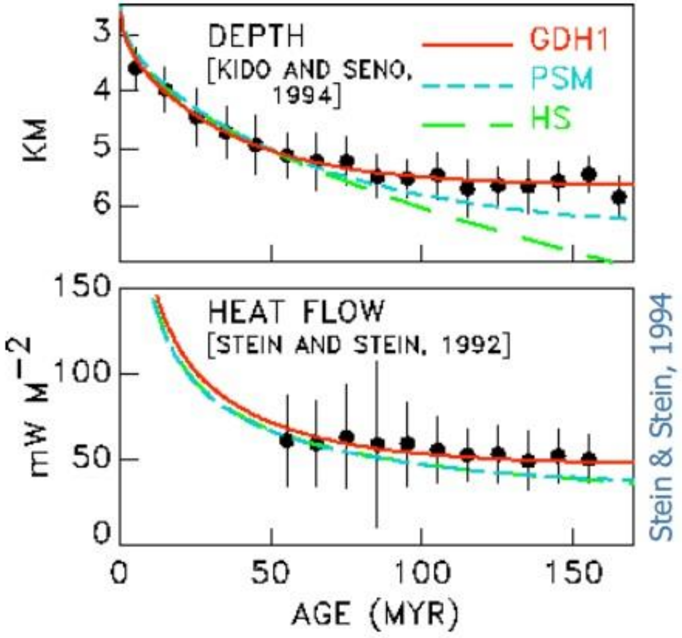

HS – Half-space model
GDH1 – plate model
PSM – plate model

The GDH1 "plate" model does a better job of fitting the depth data
(which is better constrained)

All fit the heat flow data
(within error)

Thermal parameters for oceanic-lithosphere models

		GDH1	PSM	HS
L,	plate thickness (km)	95 ± 10	125 ± 10	—
T_a,	temperature at base of plate (°C)	1450 ± 100	1350 ± 275	1365 ± 10
α,	coefficient of thermal expansion (°C^{-1})	3.1×10^{-5}	3.28×10^{-5}	3.1×10^{-5}
k,	thermal conductivity (W m^{-1})	3.138	3.138	3.138
c_P,	specific heat (kJ kg^{-1})	1.171	1.171	1.171
κ,	thermal diffusivity (m^2 s^{-1})	0.804×10^{-6}	0.804×10^{-6}	0.804×10^{-6}
ρ_m,	mantle density (kg m^{-3})	3330	3330	3330
ρ_w,	water density (kg m^{-3})	1000	1000	1000
d_r,	ridge depth (km)	2.6	2.5	2.6

for $\tau < 20$ Myr $\quad d=2.6+0.365t^{1/2}$

for $\tau > 20$ Myr $\quad d=5.65-2.47e^{-t/36}$

for < 55 Myr $\quad Q=510t^{-1/2}$

for >55 Myr $\quad Q=48+96e^{-t/36}$

Oceanic cooling models

- **If the same plate thickness is used for the flux and temperature boundary conditions, for fixed heat flux conditions the re-equilibration time is much longer than for fixed temperature conditions.**

Variation of depth and heat flow with age for oceanic-lithosphere models

	Ocean depth (km)	Heat flow (mW m^{-2})
Half-space	$2.6 + 0.345t^{1/2}$	$480t^{-1/2}$ < 80Myr
PSM	$2.5 + 0.350t^{1/2}$, $t < 70$ Ma	$473t^{-1/2}$, $t < 120$ Ma
	$6.4 - 3.2e^{-t/62.8}$, $t > 70$ Ma	$33.5 + 67e^{-t/62.8}$, $t > 120$ Ma
GDH1	$2.6 + 0.365t^{1/2}$, $t < 20$ Ma	$510t^{-1/2}$, $t < 55$ Ma
	$5.65 - 2.47e^{t/36}$ $t > 20$ Ma	$49 + 96e^{-t/36}$, $t > 55$ Ma

Different estimates of the parameters of the oceanic cooling model

ΔT (°C)	a (km)	Method	Reference
1370	–	bathymetry (age < 80 My)	
		Half-space model	Johnson and Carlson (1992)
1333	125	Constant properties – fixed T	Parsons and Sclater (1977)
1450	95	Constant properties – fixed T	Stein and Stein (1992)
1350	118	T-dependent properties	
		fixed Q at variable depth†	Doin and Fleitout (1996)
1315	106	T-dependent properties – fixed T	McKenzie *et al.* (2005)

† In this model, heat flux is fixed at the base of the growing thermal boundary layer.

Plate Cooling model vs Half-Space cooling model

A hybrid?

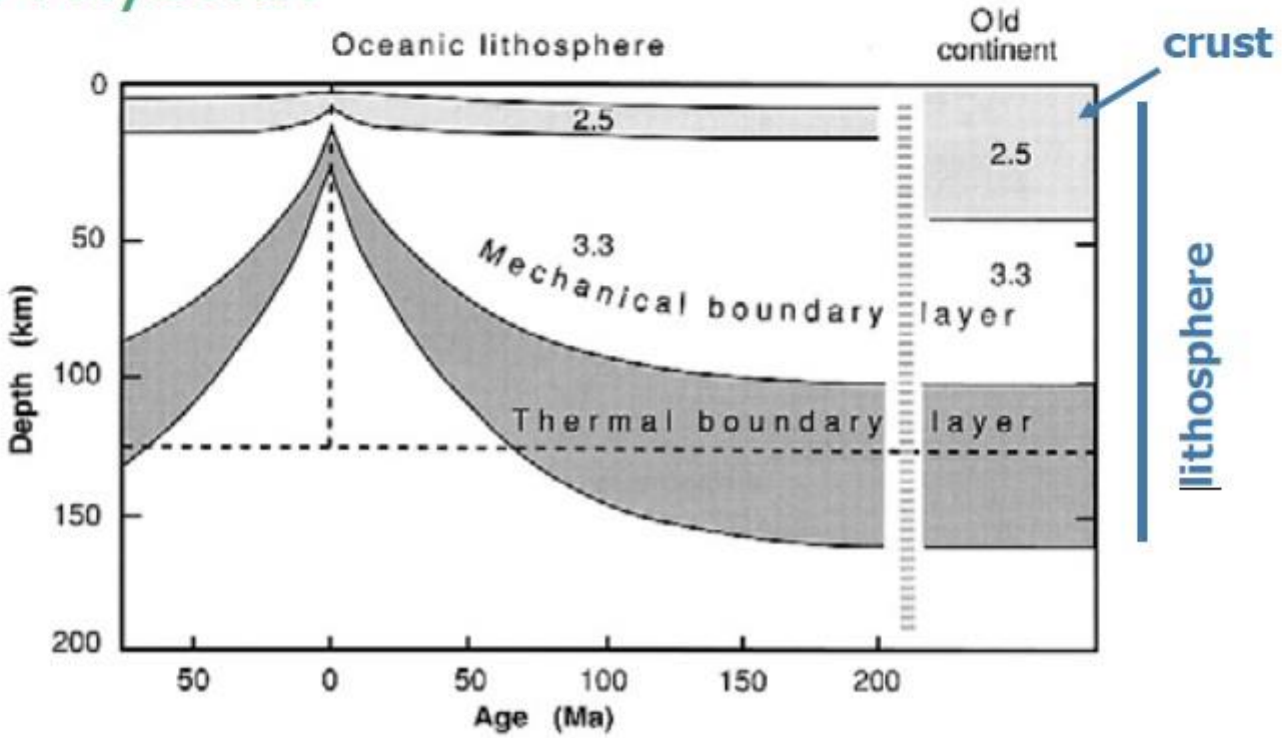

"Plate" model fits depth and Q best

but there is other geophysical evidence for a thickening lithosphere

- increasing elastic thickness
- increasing depth to low velocity asthenosphere

➔ thermal boundary layer with small-scale convection

Oceanic depth and heat flow data variations with age

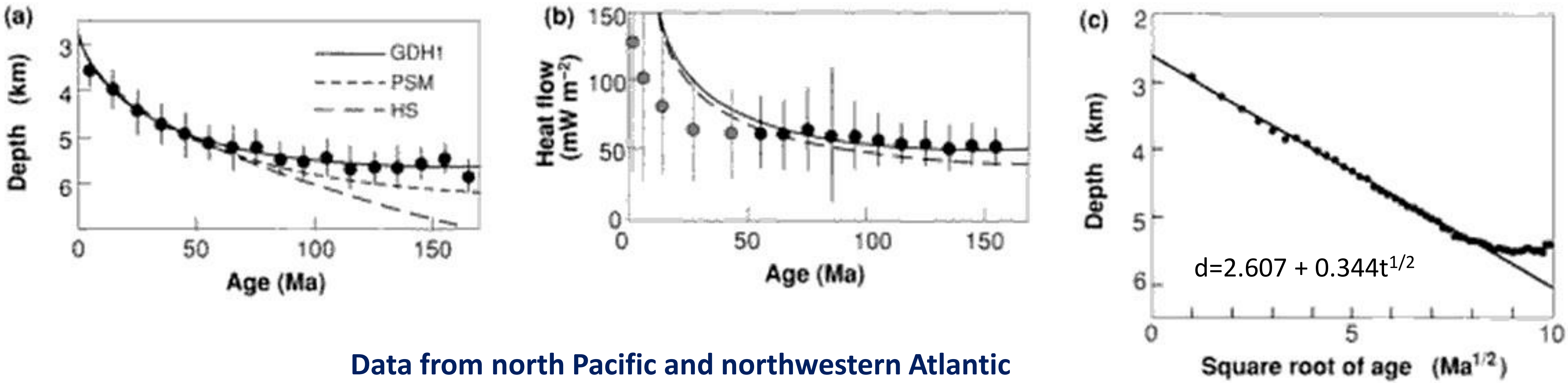

Data from north Pacific and northwestern Atlantic
(in grey data < 50Myr affected by hydrothermal circulation)

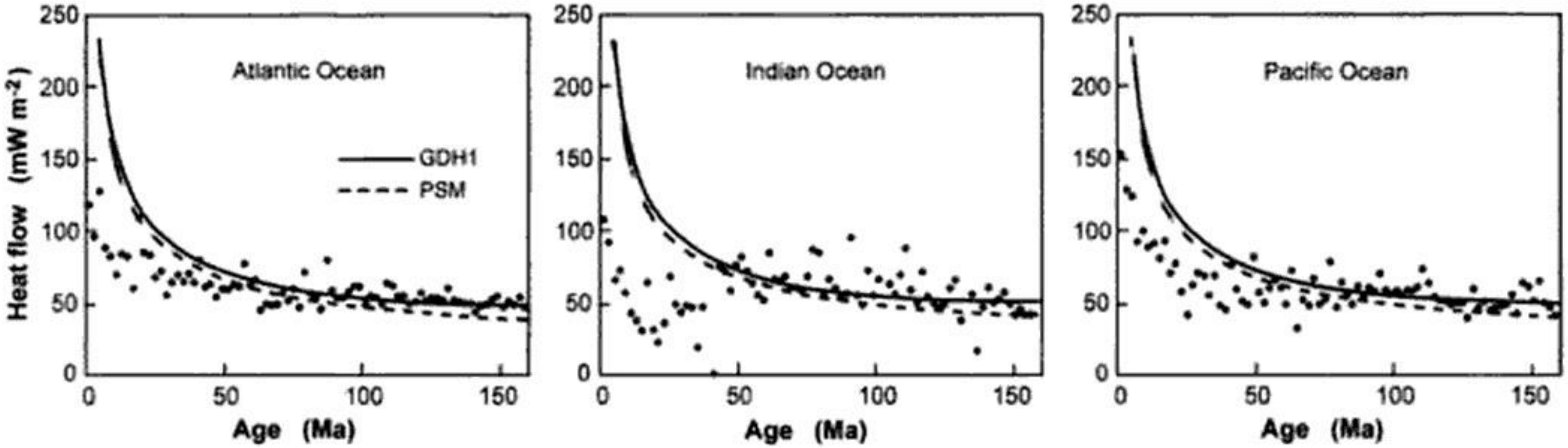

Effects of sperading rates of Mid-Ocean ridges

Mid-ocean ridges with high spreading rates (> 5 cm/yr)

- Axial high up to 400 m in height and 1-2 km wide. A central graben structure is missed.
- Tectonic extension plays a minor role (more volume of ductile crust).
- High melt production (large magma chamber), about 20 % fills up the valley and equalize the relief (smooth topography)
- Harzburgite is present in the upper lithosphere.

Mid-ocean ridges with low spreading rates (< 5 cm/yr)

- A central graben structure with steep flanks, up to 5 km deep, is present.
- Extensional tectonics is dominant (more volume of brittle crust)
- Low melt production (small magma chamber), between 10%-15% .
- Depleted lherzolite is present in the upper lithosphere.

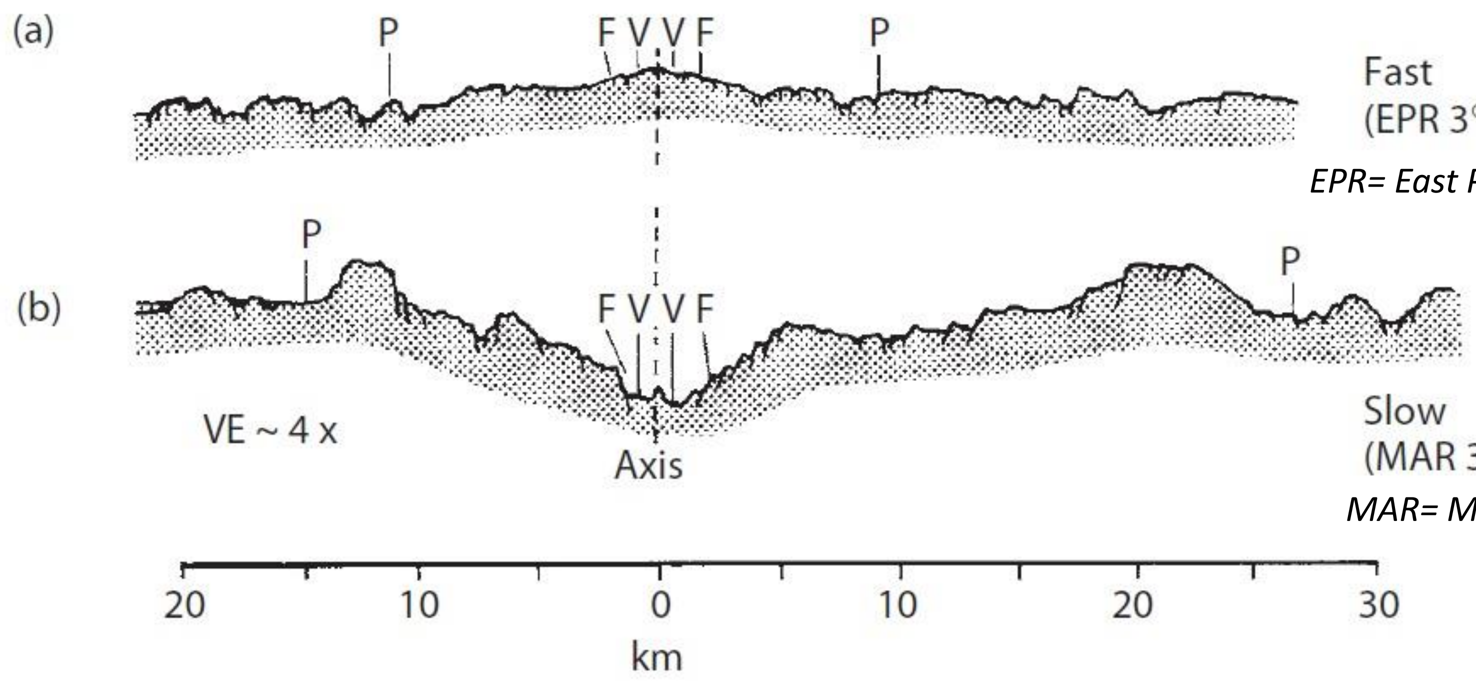

EPR= East Pacific Rise

MAR= Mid-Atlantic Ridge

Other effects of spreading rates of Mid-Ocean ridges

Mid-ocean ridges with high spreading rates (> 5 cm/yr)

- Whole crestal region at shallow depth is hot and a steady state of the magma chamber exists.
- Brittle-ductile transition occurs at shallower depth (volume of ductile is larger).

Mid-ocean ridges with low spreading rates (< 5 cm/yr)

- Lower rate of magma supply enables the crust to cool by conduction and steady state of the magma chamber cannot be mantained.
- At ultra-slow spreading ridges (Gakkel ridge) conductive cooling extends into the mantle and inhibits melt generatrion (reduction of crustal thickness).
- Abundance of serpentinites.

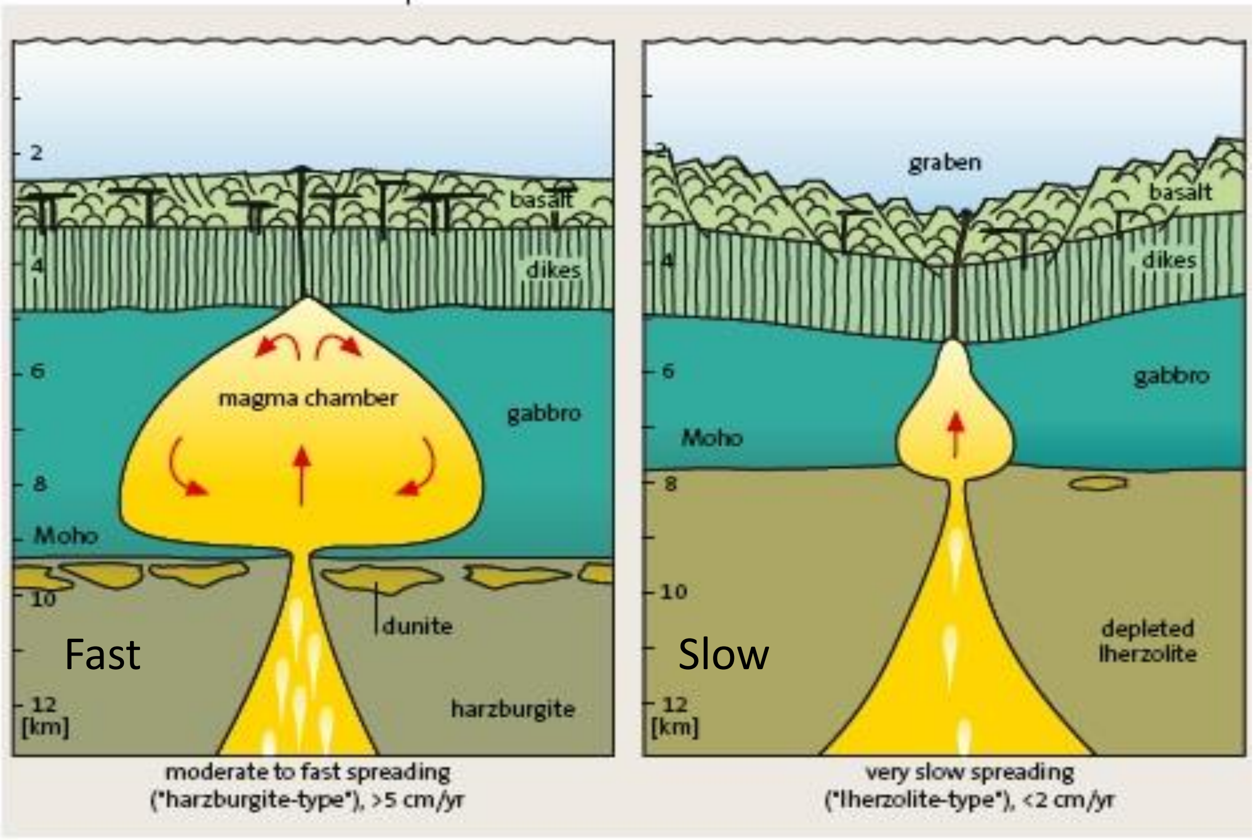

Oceanic transform faults

- Transform faults can connect two segments of growing plate boundaries (R-R transform fault), one growing and one subducting plate boundary (R-T transform fault), or two subducting plate boundaries (T-T transform fault); R stands for mid-ocean ridge, T for deep sea trench (subduction zone).
- At these faults there is neither creation nor destruction of lithosphere, but rather the motion is strike-slip, with adjacent lithosphere in tangential motion.
- The term ‘transform fault’ was given because the lateral displacement across the fault is taken up by transforming it into either the formation of new lithosphere at a terminated ocean ridge segment or lithosphere subduction at a trench.
- These faults are well defined by fracture zones, which are long, linear, bathymetric depressions that normally follow arcs of small circles on the Earth’s surface perpendicular to the offset ridge. These multifaults zones are wider and more common on fast-spreading ridges (e.g., the East Pacific Rise).
- Serpentinite intrusion is quite common within fracture zones, accompanied by alkali basalt volcanism, hydrothermal activity, and metallogenesis.
- The transcurrent, or strike-slip, fault causes a sinistral offset along a vertical plane which must stretch to infinity beyond the ridge crests.
- The transform fault is only active between the offset ridge crests, and the relative movement of the lithosphere on either side of it is dextral.

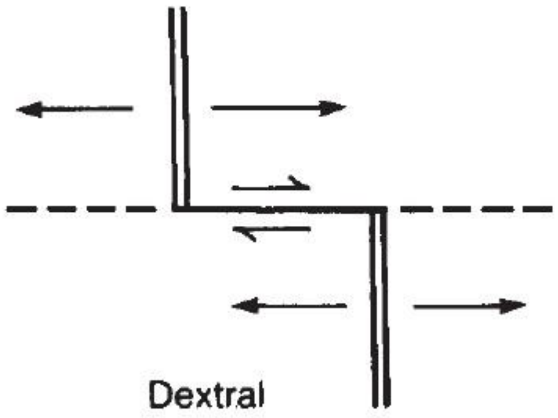

(a) Transform fault

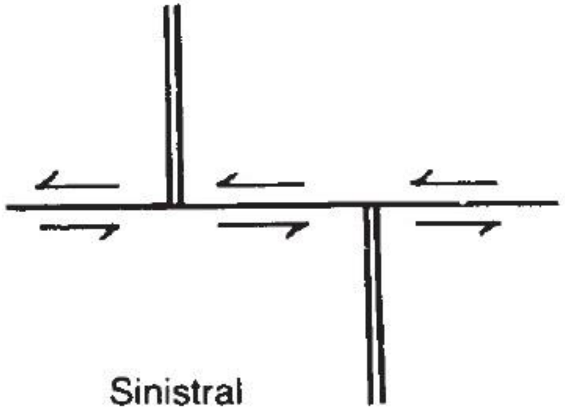

(b) Transcurrent fault

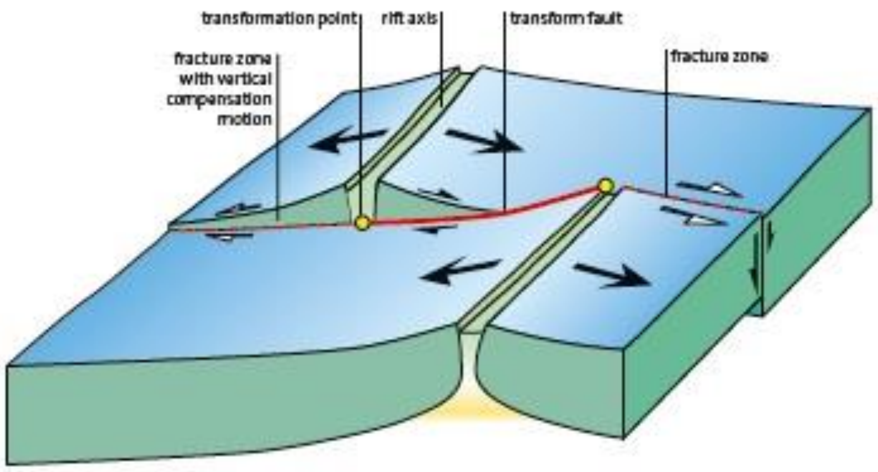

Oceanic transform faults

- There are six classes of transform fault that depend upon the types of non conservative features they join. These may be an ocean ridge, the overriding plate at a trench or the underthrusting plate at a trench.
- How the transform faults would develop with time. Cases (i) and (v) will remain unchanged, cases (ii) and (iv) will grow, and cases (iii) and (vi) will diminish in length with time.

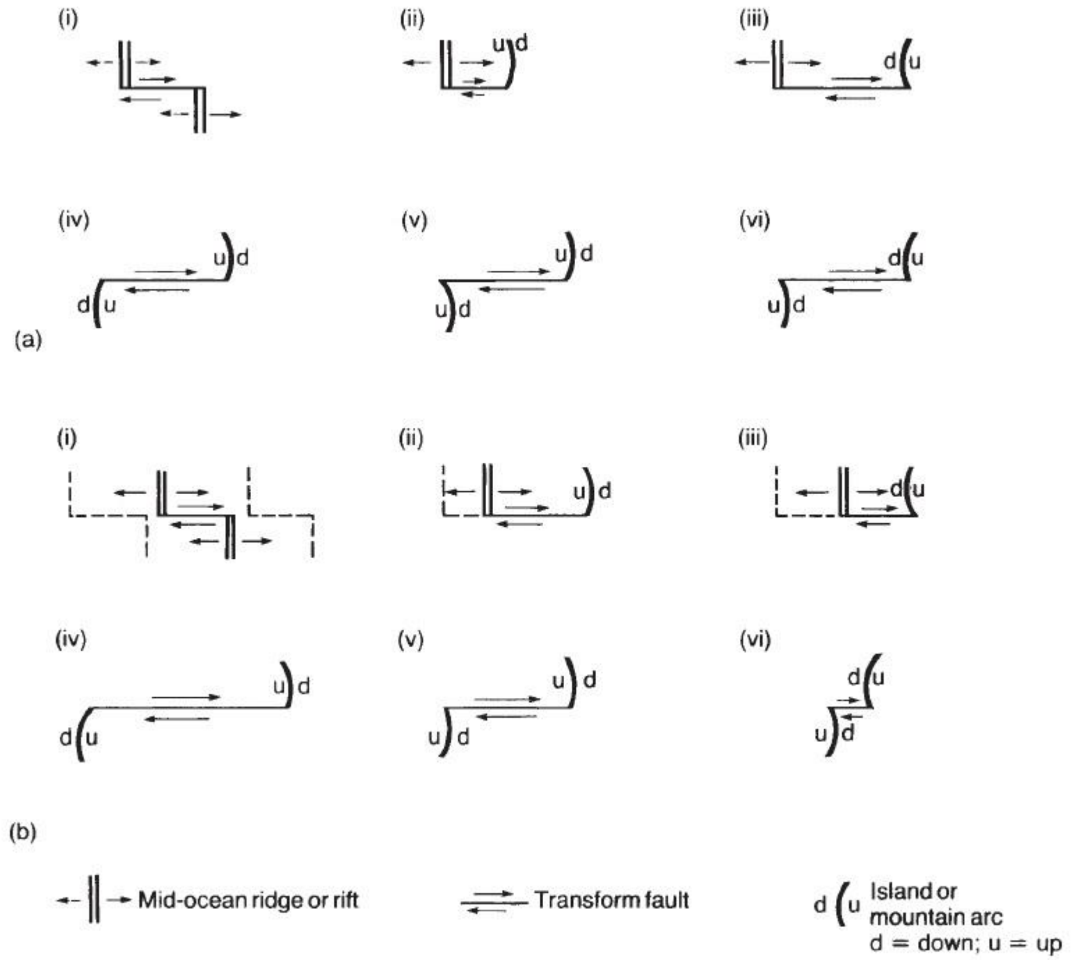

(a) Six possible types of dextral transform fault: (i) ridge to ridge; (ii) ridge to concave arc; (iii) ridge to convex arc; (iv) concave arc to concave arc; (v) concave arc to convex arc; (vi) convex arc to convex arc. (b) Appearance of the dextral transform faults after a period of time.

Slow-spreading and fast-spreading ridge

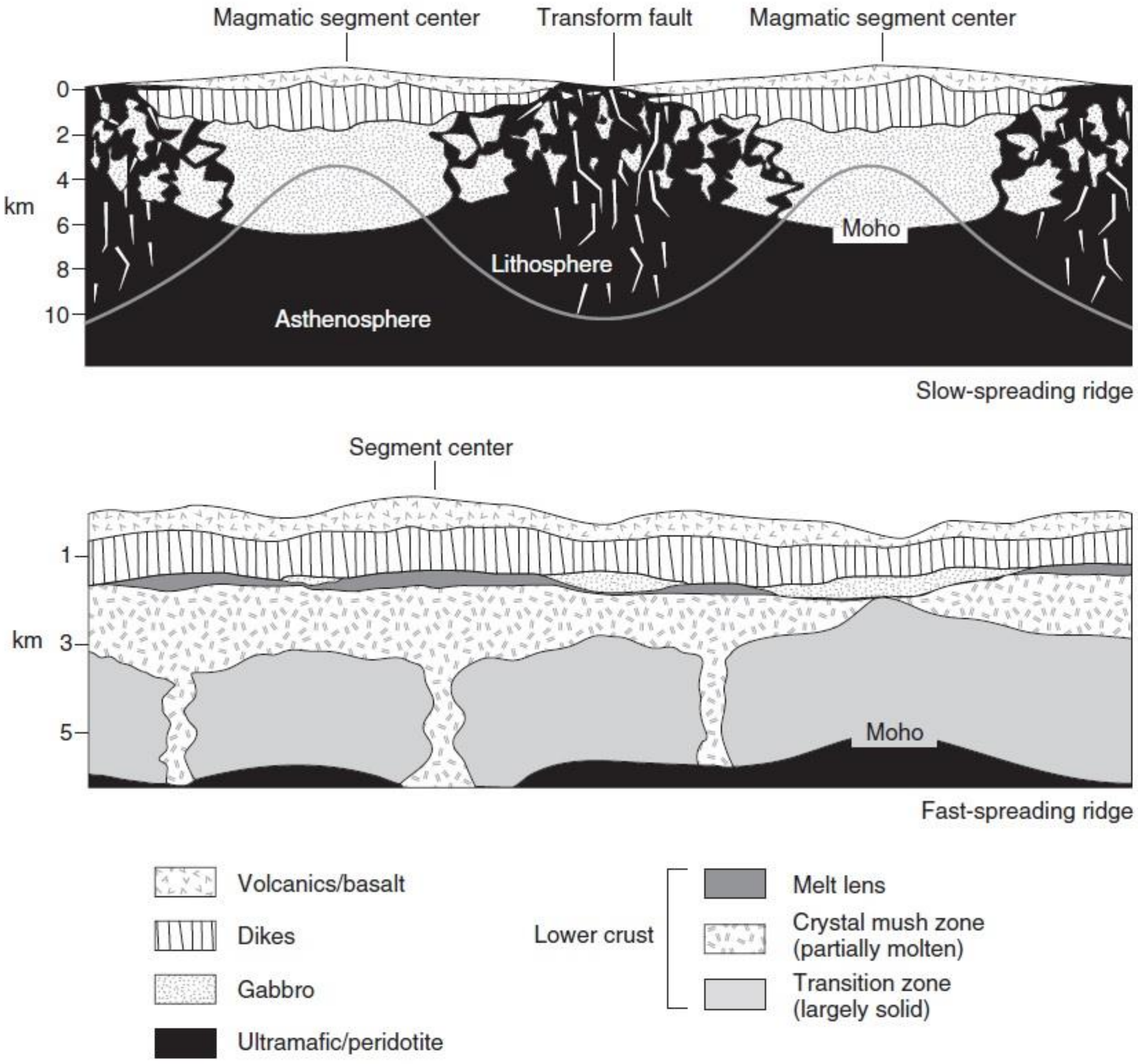

- In the slow-spreading Mid-Atlantic Ridge, the first order segment boundaries, transform faults, are marked by pronounced bathymetric depressions.
- They are often underlain by thinner crust than normal and anomalously low sub-Moho seismic velocities that may be due to partial serpentinization of the mantle (due to seawater percolating down through the fractured crust).
- The central portions of segments are elevated, have crust of normal thickness, and thinner lithosphere.
- These regions of thicker crust and enhanced magma supply are characterized by negative mantle Bouguer anomalies and the areas of thinned crust between them by positive Bouguer anomalies .
- Samples along the axis of the southern Mid-Atlantic Ridge showed that there are regular patterns of magma chemical variation along it, caused by differences in the depth and extent of partial melting and degree of fractionation.

Slow-spreading and fast-spreading ridge

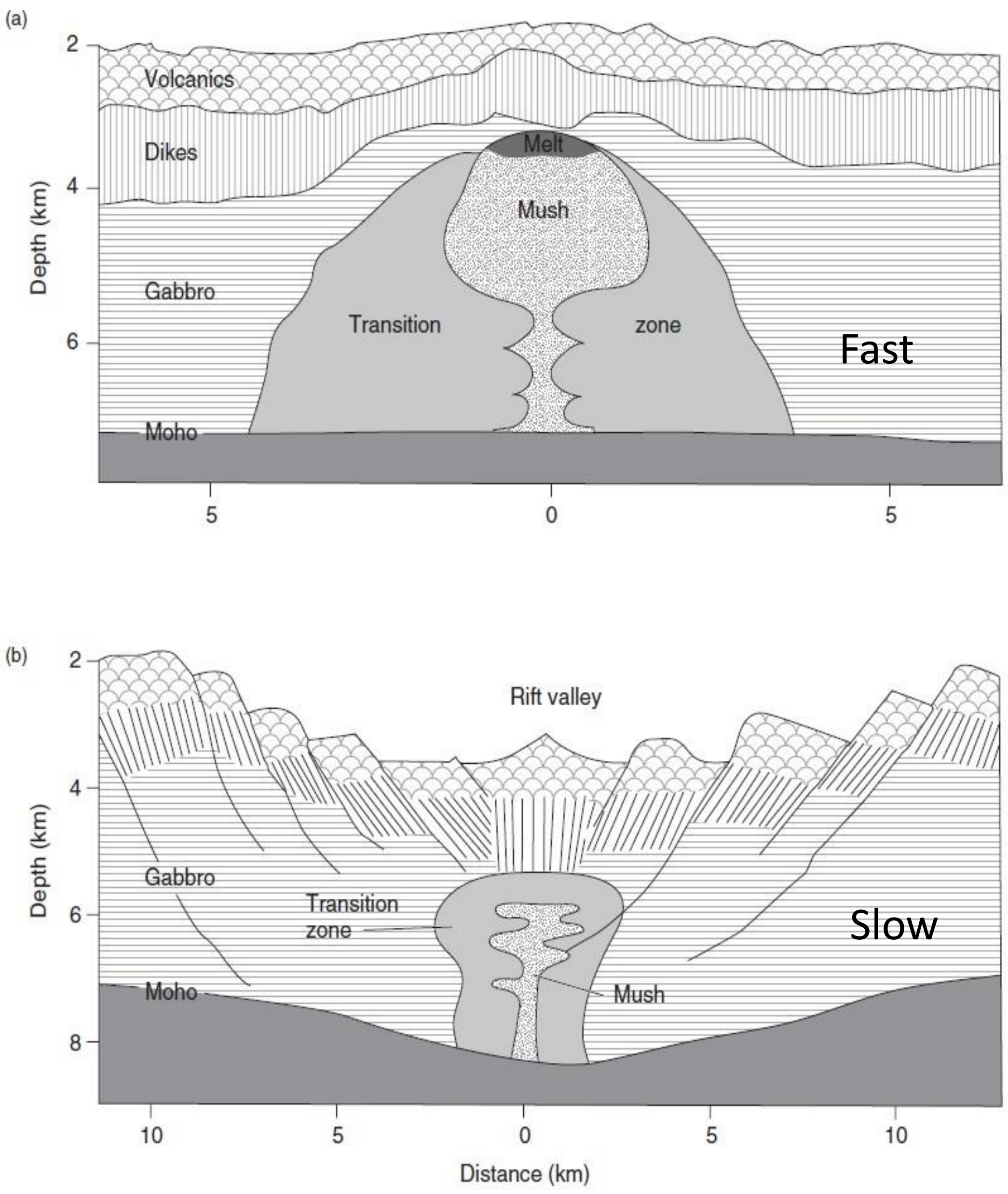

- Fast-spreading ridges suggest low-pressure basalt fractionation trends to iron-rich compositions with little plagioclase accumulation or crystal–liquid interaction. This is consistent with the magma chamber being a stable and steady state feature.
- Basalts from very slow- and ultraslow-spreading ridges have lower *Na* and higher *Fe* contents than typical MORB, reflecting a smaller degree of mantle melting and melting at greater depths.
- The great variation in the rate at which magma is supplied along the length of the ultra-slow Gakkel Ridge is effect of the smaller vertical extent of melting (*T* variations) beneath this ridge.
- On fast spreading ridges the magma supply rate is such that the whole crustal region at relatively shallow depth is kept hot (cools for the effect of hydrothermal circulation) and a steady state magma chamber exists.
- On slow-spreading ridges the lower rate of magma supply enables the crust to cool by conduction, as well as hydrothermal circulation. Thus, a steady state magma chamber or even transient cannot be maintained.
- At spreading rates of less than 20 mm yr^{-1} this conductive cooling between injections of magma extends into the mantle and inhibits melt generation. This reduces the magma supply, as well as the thickness of mafic crust.

Slow-spreading and fast-spreading ridge

- The geometry of the fast-spreading ridge structure indicates a very narrow and persistent zone of dike intrusion, and isostatic subsidence as the thickness of the lava flow unit increases away from the point of extrusion.
- In the slow-spreading ridges more brittle upper crust, extension by normal faulting is more pronounced, as a result of less frequent eruptions of magma and a cooling.
- Very slow-spreading ridges are characterized by a wider zone of crustal accretion, thin mafic crust, and large regions of peridotite exposures.

Fast-Spreading Ridge

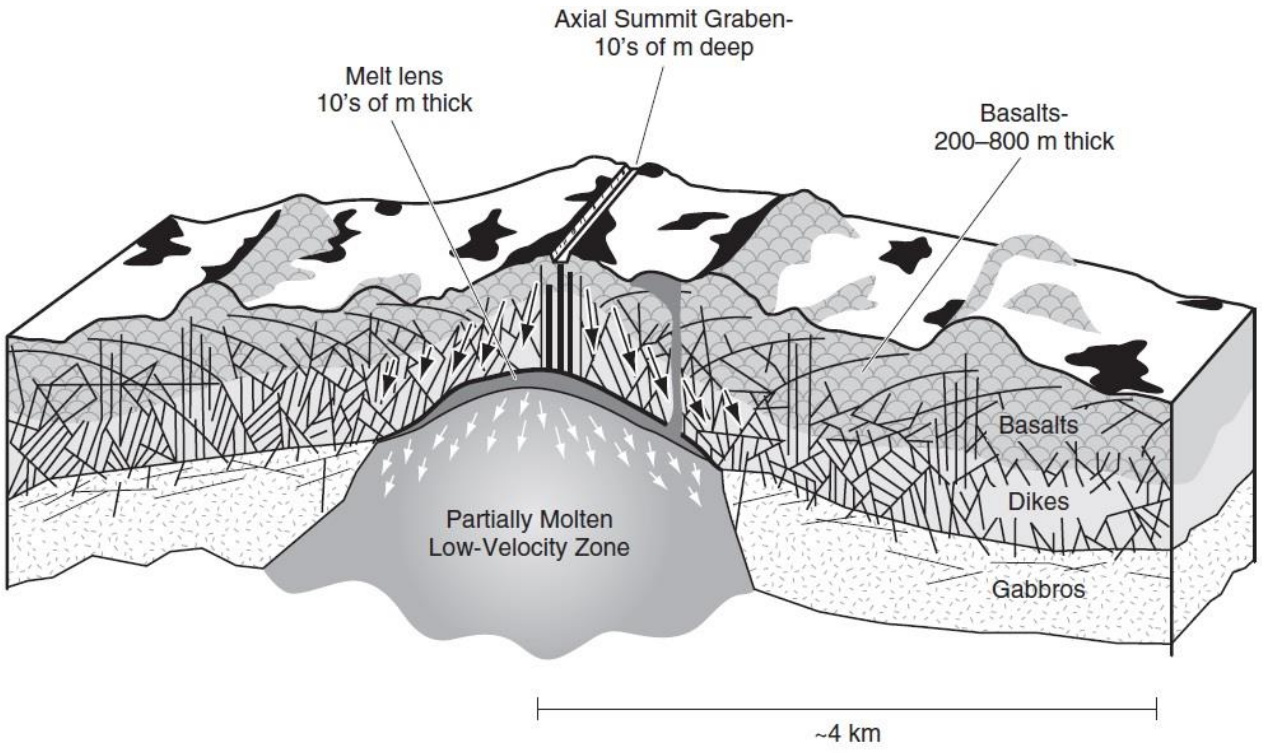

Slow-spreading and fast-spreading ridge

- The thermal regime beneath a ridge crest is influenced by the rate at which magma is supplied to the crust, which depends on the spreading rate.
- As a consequence the brittle–ductile transition (at ~750°C) occurs at a shallower depth in the crust at a fast-spreading ridge compared to a slow-spreading ridge that has a lower rate of magma supply.
- This in turn implies that at a fast-spreading ridge there is a much greater volume, and hence width, of ductile lower crust, which decouples the overlying brittle crust from the viscous drag of the convecting mantle beneath (tensile stress concentrated in a narrow area at the ridge axis).
- On a slow-spreading ridge the brittle layer is thicker and the volume of ductile crust is much smaller (the tensile stress is distributed over a larger area).
- The transition from smooth topography with a buoyant axial high to a median rift valley is quite abrupt, at a full spreading rate of approximately 70 mm/yr.

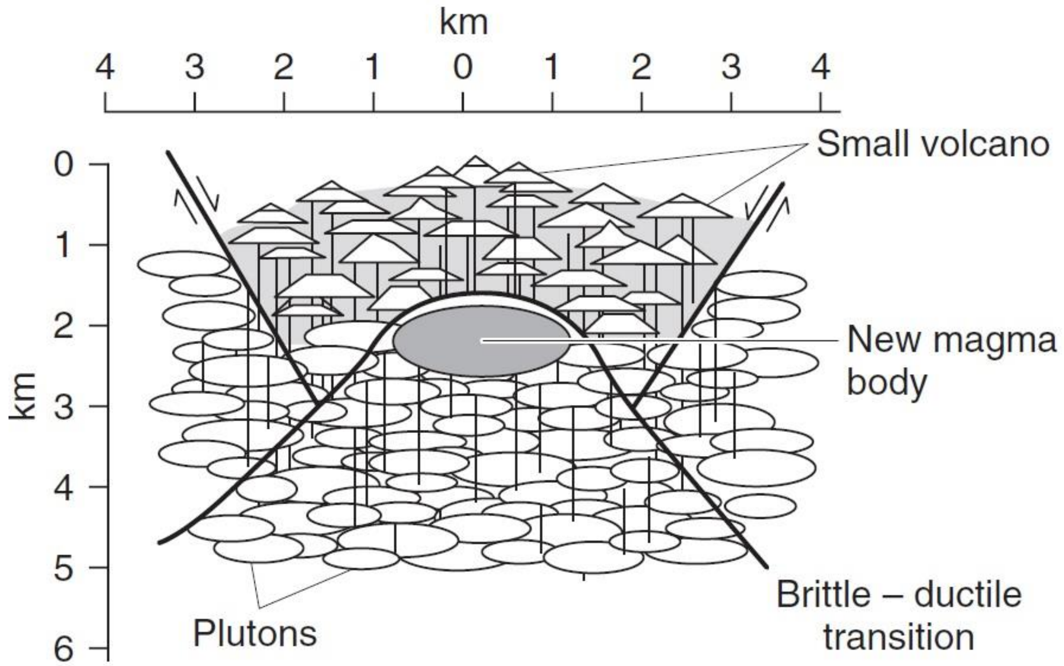

Segmentation of Oceanic Ridges

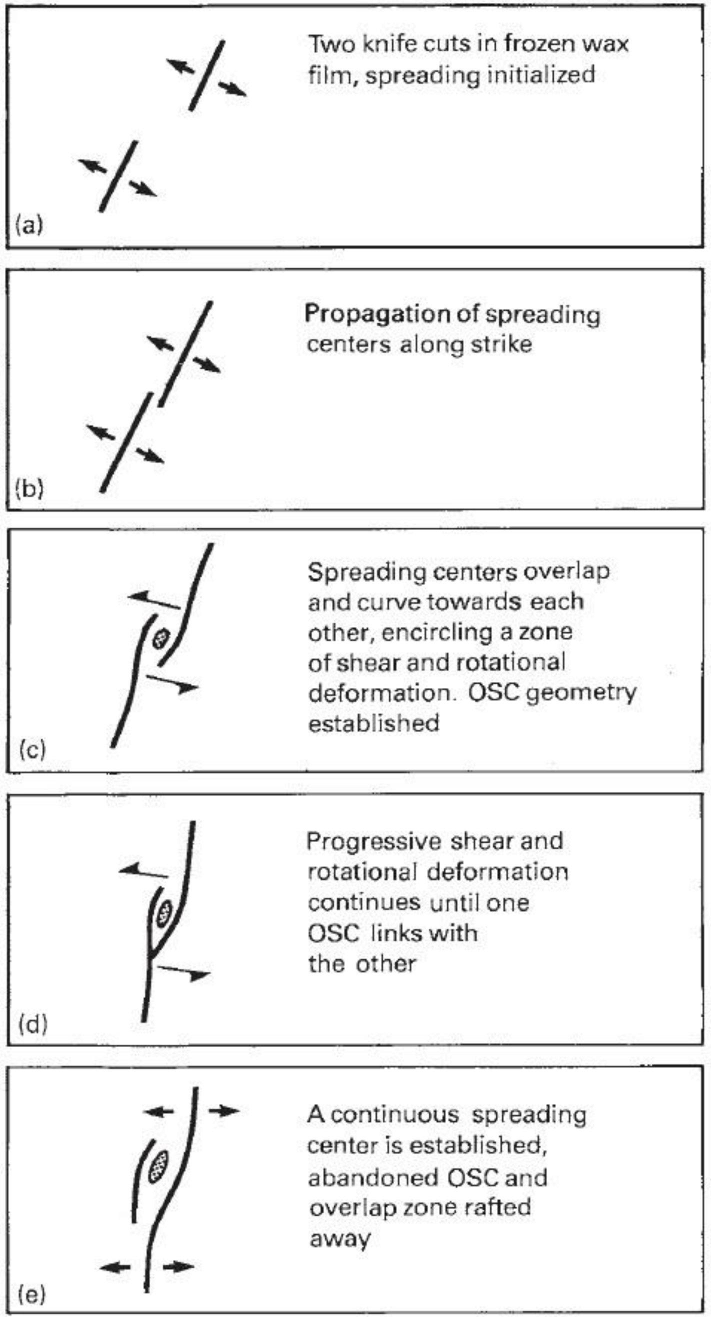

- Studies of the fast-spreading East Pacific Rise shown that it is segmented along its strike by **nontransform ridge axis discontinuities** such as propagating rifts and **overlapping spreading centers** (OSC), which occur at local depth maxima, and by smooth variations in the depth of the ridge axis.
- OSCs are nonrigid discontinuities where the spreading center of a ridge is offset by a distance of 0.5–10 km, with the two ridge portions overlapping each other by about three times the offset. OSCs originate on fast-spreading ridges where lateral offsets are less than 15 km, and true transform faults fail to develop because the lithosphere is too thin and weak.
- Tension applied orthogonal to the spreading centers causes their lateral propagation until they overlap, and the enclosed zone is subjected to shear and rotational deformation. The OSCs continue to advance until one tip links with the other OSC. A single spreading center then develops as one OSC becomes inactive and is moved away as spreading continues.

Segmentation of Oceanic Ridges

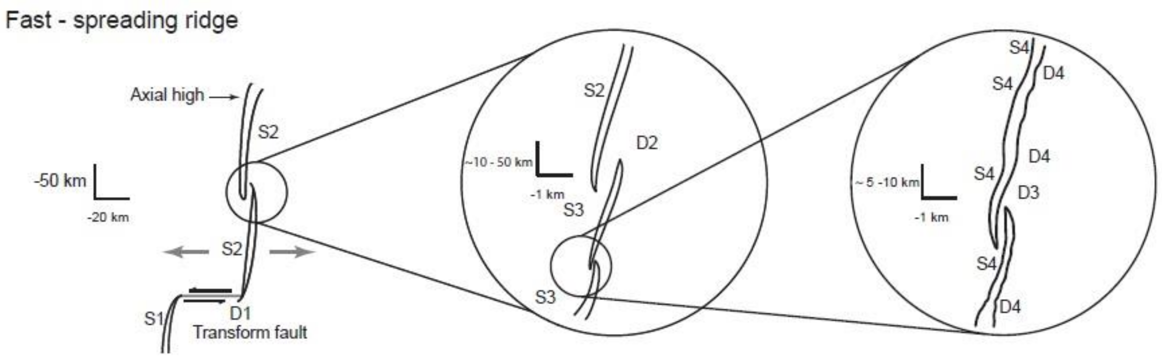

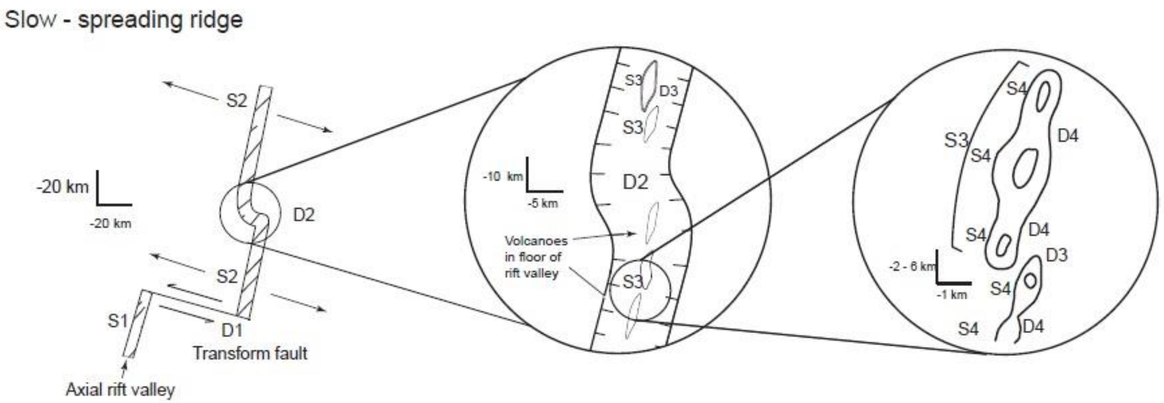

Fast-spreading ridges are segmented at several different scales:

- **First order segmentation** is defined by fracture zones (and propagating rifts), which divide the ridge at intervals of 300–500 km by large axial depth anomalies.
- **Second order segmentation** at intervals of 50–300 km is caused by nonrigid transform faults (which affect crust that is still thin and hot) and large offset (3–10 km) OSCs that cause axial depth anomalies of hundreds of meters.
- **Third order segmentation** at intervals of 30–100 km is defined by small offset (0.5–3 km) OSCs, where depth anomalies are only a few tens of meters.
- **Fourth order segmentation** at intervals of 10–50 km is caused by very small lateral offsets (<0.5 km) of the axial rift and small deviations from axial linearity of the ridge axis (DEVALS). These are may be represented by gaps in the volcanic activity within the central rift or by geochemical variation.
- **Third and fourth order segmentations appear to be short-lived**. Second order segmentations, create off axis scars on the spreading crust forming V-shaped wakes at 60–80° to the ridge, indicating that the OSCs migrate along the ridge at velocities of up to several hundred mm/yr.
- First to third order segmentation is caused by the variable depth associated with magma migration, while fourth order effects are caused by the geochemical differences in magma supply.

Propagating Rifts

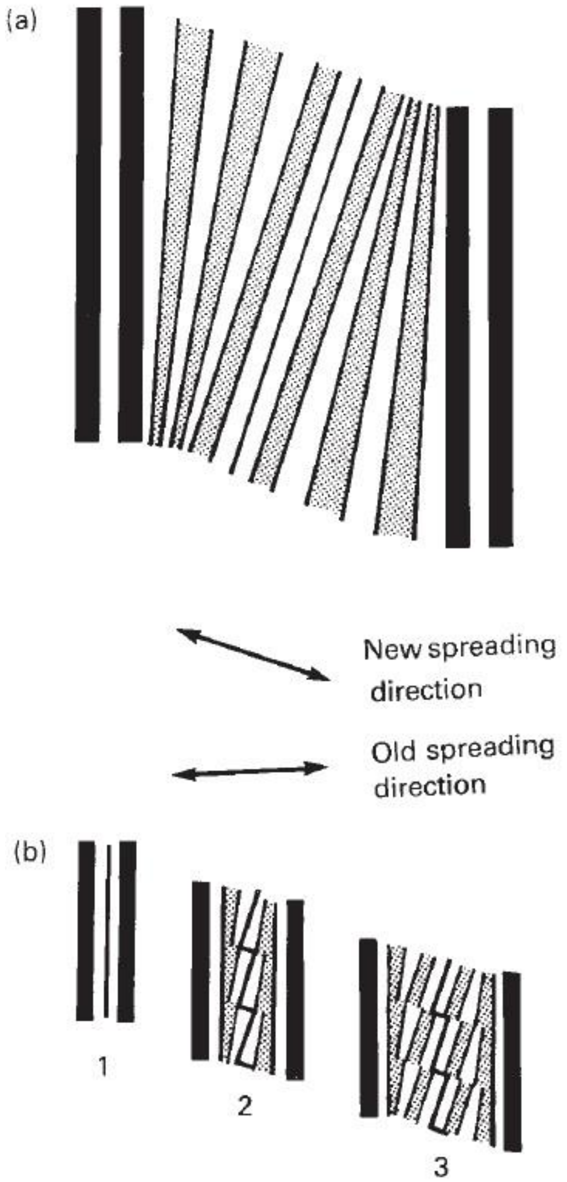

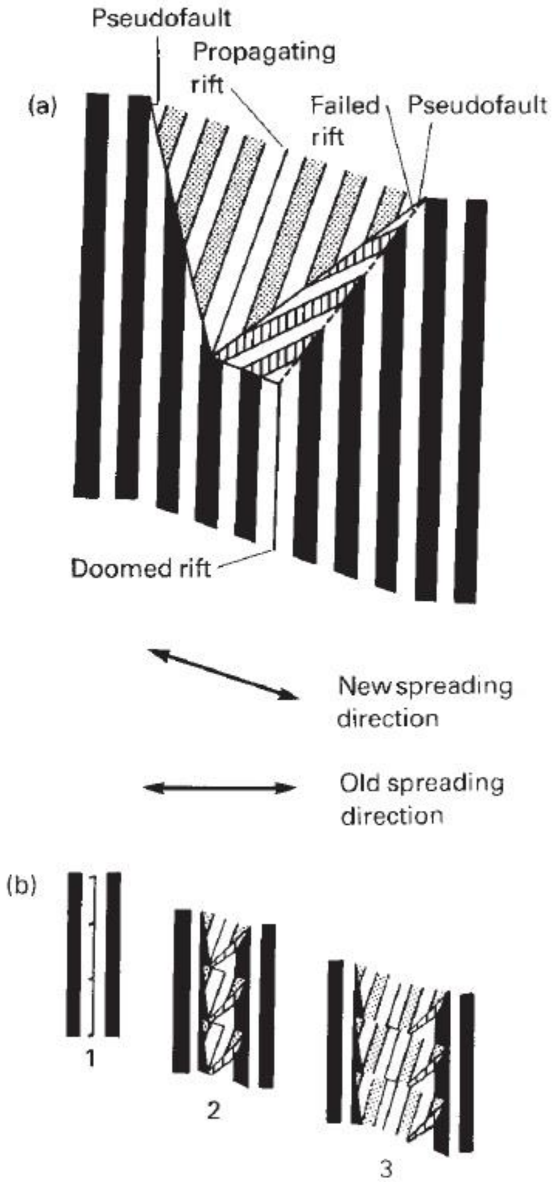

- The direction of spreading at an ocean ridge may undergo several small changes: e.g., spreading in the northeastern Pacific had changed direction five times on the basis of changes in the orientation of major transform faults and magnetic anomaly patterns.
- The reorientation of a ridge would take place by smooth, continuous rotations of individual ridge segments until they became orthogonal to the new spreading direction.
- The change in spreading direction occurs as a gradual, continuous rotation that produces a fan-like pattern of magnetic anomalies that vary in width according to position.
- The old rift is progressively replaced by a propagating spreading center orthogonal to the new spreading direction.
- Between the propagating and failing rifts, lithosphere is progressively transferred from one plate to the other, giving rise to a sheared zone with a quite distinctive fabric.
- The rotation model predicts a continuous fanlike configuration of magnetic anomalies whose direction changes from the old to new spreading direction.

Propagating Rifts

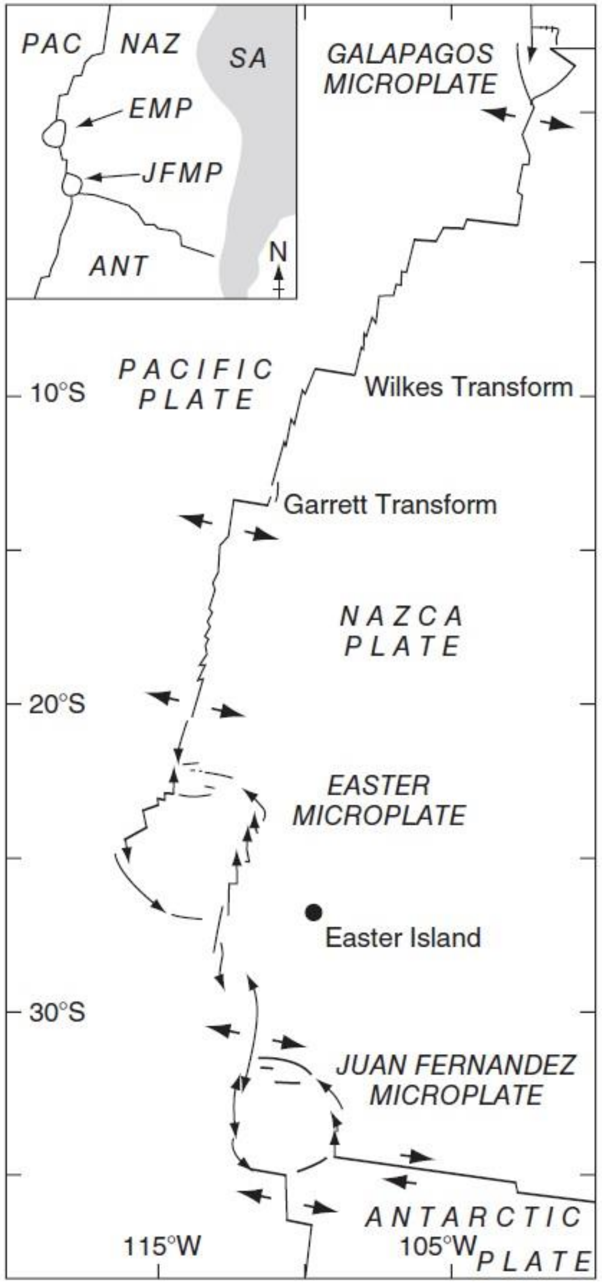

- If spreading on the new rift started at a slow rate, and only gradually increases over a period of Myrs, the failing rift continues to spread, in order to maintain the net accretion rate. The two rifts overlap and the area of oceanic lithosphere between them increases with time.
- As a result of the gradients in spreading rate along each rift, the block of intervening lithosphere rotates, producing compression in the oceanic lithosphere adjacent to the tip of the propagating rift and transtension in the region between the points where the propagating rift was initiated and the original rift started to fail.
- These processes cause the formation of microplates, which usually exist for less than 5–10 Myr, by which time the initial rift succeeds in transferring the oceanic lithosphere of the microplate from one plate to another.